

Investigating the Role of Disulfide Bond Formation in FABP5

Author: Katie Love

Persistent link: <http://hdl.handle.net/2345/bc-ir:107265>

This work is posted on [eScholarship@BC](#),
Boston College University Libraries.

Boston College Electronic Thesis or Dissertation, 2016

Copyright is held by the author. This work is licensed under a Creative Commons Attribution-NonCommercial-NoDerivatives 4.0 International License (<http://creativecommons.org/licenses/by-nc-nd/4.0>).

INVESTIGATING THE ROLE OF DISULFIDE BOND FORMATION IN FABP5

Katie Love

A thesis

submitted to the Faculty of

the department of the Graduate School of the Morrissey College of Arts and Sciences

in partial fulfillment

of the requirements for the degree of

Master of Science

Boston College
Morrissey College of Arts and Sciences
Graduate School

Investigating the Role of Disulfide Bond Formation in FABP5

By: Katie Lynn Love

Thesis Advisor: Professor Eranthie Weerapana

Abstract:

EGF signaling activates multiple pathways within the cell that lead towards proliferation, rendering this pathway of interest for cancer therapy. Recent studies focused on triple-negative breast cancer have shown that EGF-induced tumorigenesis strongly correlates with the up-regulation of FABP5, which shuttles fatty acids from the cytoplasm of cells to the nucleus. Our work began with the identification of redox active cysteine residues upon EGF activation *in situ* using a caged electrophile to perform live cell labeling. In these studies, the C120 residue of FABP5 was identified as a cysteine with high redox activity and thus became a subject of further interest. The characterization of redox active cysteine residues yields important information about protein structure and function. We have confirmed these results via in-gel fluorescence and developed fluorescence assays to probe the significance of C120 and C127 in FABP5. Two fatty acids were chosen based on their conformation in the FABP5 binding pocket. Upon the addition of a fatty acid, wild type protein showed a decrease in fluorescence indicating that the fatty acids were outcompeting the fluorophores used. Future studies will investigate both wild type and mutant versions of FABP5 with emphasis on determining potential disulfide bond formation via phosphoproteomics and western blotting techniques.

Acknowledgement

First I would like to thank Professor Eranthie Weerapana for the opportunity to work in her laboratory and explore chemical biology. My personal goal for graduate school, to broadly expand my toolkit, has been met with this project. I would also like to thank current and previous laboratory members for their assistance and guidance during my time here.

Secondly, I want to thank my mentors at the University of Massachusetts Amherst, in particular Professor Richard Vachet, for their continued encouragement. Your unbiased counseling has been invaluable in this process and I deeply appreciate it. Knowing that I have your full support with my career endeavors gives me added confidence in pursuing my interests.

I'd also like to thank the many friends who supported me through this trying process. In particular Allison Young for our walks around the reservoir for some fresh air, Lauren Blair for your abundant optimism, Jill Graham for our many coffee dates, and Jessica Weber for exploring Boston with me. The ability to talk freely and expect an honest opinion in return is rare and I value your candor. To all of my friends, I am fortunate to know so many good people and I hope you feel that I've shown the same level of support and inspiration to each of you.

Finally I would like to thank my family, especially my mom and sister. It has been so convenient to visit home during particularly difficult times and your love and support have carried me through this experience. I cannot thank you enough. You are both loved tremendously and I know that no matter where life takes me, you'll always cheer me on. Know that I will always be there for you wherever I go.

Table of Contents

List of Figures.....	iv
List of Tables.....	v
List of Abbreviations.....	vi

Chapter 1: Introduction

1.1 Epidermal Growth Factor Signaling.....	1
1.1.1 Pathway and Cancer Relevance.....	1
1.1.2 Production of Reactive Oxygen Species.....	8
1.2 Role of Cysteine as it Relates to Reactive Oxygen Species.....	10
1.2.1 Cysteine Oxidation and Disulfide Bond Formation.....	10
1.2.2 Monitoring Cysteine Reactivity in Living Cells.....	12
1.3 Fatty Acid Binding Protein 5.....	16
1.3.1 Fatty Acid Binding Protein Family.....	16
1.3.2 Cellular Function and Cancer Relevance.....	20
1.3.3 Binding Pocket and the Relevance of Cysteine Residues.....	23
1.4 Experimental Goals.....	25

Chapter 2: Experiments and Results

2.1 Recombinant Expression of WT and Mutant FABP5.....	26
2.2 Development of Fluorescence Assays.....	28
2.3 Expression of FABP5 in Mammalian Cells.....	37

Chapter 3: Conclusions and Future Directions

3.1 Summary of Results and Conclusions.....	38
3.2 Future Directions.....	38

3.2.1 Transfections into Mammalian Cells.....	38
3.2.2 Phosphoproteomics.....	40
3.2.3 Western Blotting.....	44

Chapter 4: Materials and Methods

4.1 Cloning and Mutagenesis.....	50
4.2 Bacterial and Mammalian Cell Culture.....	59
4.3 Analytical Methods.....	63
<i>References</i>	69

List of Figures

1.1 EGF signaling via the PI3K/AKT pathway.....	2
1.2 Production of hydrogen peroxide as it relates to EGF signaling.....	8
1.3 Oxidative PTMs of cysteine residues.....	11
1.4 Use of Iodoacetamide alkyne to probe the proteome analyzed by in-gel fluorescence and mass spectrometric methods.....	13
1.5 Caged electrophile for live cell labeling and analysis via mass spectrometry.....	14
1.6 Results comparing cysteine oxidation in cells with and without EGF stimulation.....	15
1.7 Sequence homology between FABP family members.....	17
1.8 Relevance of FABP5 in retinoic acid signaling pathway.....	21
1.9 Crystal structure of FABP5 bound to linoleic acid (PDB: 4LKT).....	23
2.1 Coomassie images of the purification of WT and all mutant FABP5 overexpression large-scale growths.....	26
2.2 Coomassie image of purified WT and all mutant FABP5.....	27
2.3 Evaluating fluorophores for FABP5 fluorescence assays.....	29
2.4 Assay type 1 with WT and all mutant FABP5.....	31
2.5 Assay type 2 with WT and C120/127S FABP5.....	33
2.6 Assay type 3 with WT and all mutant FABP5.....	35
2.7 Expression of FABP5 in Mammalian Cells.....	37
3.1 Workflow for phosphoproteomics studies.....	41
3.2 Western Blot technique to monitor protein phosphorylation.....	45

List of Tables

3.1 List of available antibodies for both phosphorylated and non-phosphorylated components of the EGF signaling pathway.....	46-47
4.1 Primers successfully used for WT and all FABP5 mutants.....	50
4.2 Restriction digest volumes.....	52

List of Abbreviations

EGF	Epidermal Growth Factor
PI3K	Phosphatidylinositol (4,5)-bisphosphate 3-Kinase
AKT	Protein Kinase B
TGF-alpha	Transforming Growth Factor - Alpha
EGFR	Epidermal Growth Factor Receptor
PIP ₂	Phosphatidylinositol (4,5)-bisphosphate
PIP ₃	Phosphatidylinositol (3,4,5)-trisphosphate
PDK1	Phosphoinositide-dependent Kinase-1
PTEN	Phosphatase and Tensin Homologue
mTORC2	Mechanistic Target of Rapamycin Complex 2
BAX	Bcl-2-assisted X protein
TSC1-2	Complex between Tuberous Sclerosis 1 and 2
mTORC1	Mechanistic Target of Rapamycin Complex 1
RHEB	Ras homologue enriched in brain
S6K	Ribosomal Protein S6 Kinase
FOXO	Forkhead Box O3
ERBB2 (HER2)	Human Epidermal Growth Factor Receptor 2
ERBB3 (HER3)	Human Epidermal Growth Factor Receptor 3
ERBB4 (HER4)	Human Epidermal Growth Factor Receptor 4
mRNA	messenger Ribonucleic Acid
EGFRvIII	Epidermal Growth Factor Receptor variant III
ATP	Adenosine Triphosphate

NSCLC	Non-small cell lung cancer
FKBP-12	FK506 Binding Protein-12
ROS	Reactive Oxygen Species
NOX	NADPH Oxidases
H ₂ O ₂	Hydrogen Peroxide
NADPH	Nicotinamide Adenosine Dinucleotide Phosphate
PTP	Protein Tyrosine Phosphatase
Trx	Thioredoxin
Prx	Peroxiredoxin
GSH:GSSG	Ratio of reduced to oxidized glutathione
GSH	Reduced glutathione
PTM	Post Translational Modification
Grx	Glutaredoxin
IA	Iodoacetamide
UV	Ultra violet
BK	Bromo ketone
CuACC	Copper Assisted Click Chemistry
LC-MS	Liquid Chromatography-Mass Spectrometry
R _{H/L}	Heavy to Light Ratio
FABP	Fatty Acid Binding Protein
iLBP	Intracellular Lipid Binding Protein
PPAR	Peroxisome Proliferator-Activated Receptor
RBP4	Retinol Binding Protein 4

STRA6	Stimulated by Retinoic Acid 6 protein coding gene
RALDH2	Retinaldehyde Dehydrogenase 2
CRABP2	Cellular Retinoic Acid Binding Protein 2
RAR	Retinoic Acid Receptor
RXR	Retinoid X Receptor
TNF- α	Tumor Necrosis Factor Alpha
VEGF	Vascular Endothelial Growth Factor
NF- κ B	Nuclear Factor kappa-light-chain-enhancer of activated B cells
PA-FABP	Psoriasis-associated Fatty Acid Binding Protein
C-FABP	Cutaneous Fatty Acid Binding Protein
K-FABP	Keratinocyte Fatty Acid Binding Protein
PDB	Protein Databank
WT	Wild Type
IPTG	Isopropyl β -D-1-thiogalactopyranoside
1,8-ANS	1,8-Anilinonaphthalene-8-Sulfonic acid
DAUDA	11-(dansylamino)undecanoic acid
KI	Binding constant
KD	Dissociation constant
mM	Millimolar
nm	Nanometer
m/z	Mass to charge ratio
SILAC	Stable isotope labeling with amino acids in cell culture

uL	Microliter
HRP	Horseradish peroxidase
PCR	Polymerase chain reaction
mg/mL	Milligrams per milliliter
DNA	Deoxyribonucleic acid
dNTP	Deoxynucleotide triphosphate
fM	Femtomolar
uM	Micromolar
DMSO	Dimethylsulfoxide
LB	Lysogeny broth
PBS	Phosphate buffered saline
°C	Degrees Celsius
Ni	Nickel
rpm	Rotations per minute
cm	Centimeter
nM	Nanomolar
DMEM	Dulbecco's Modified Eagle Medium
RPMI	Roswell Park Memorial Institute medium
PSA	Penicillin-Streptomycin-Amphotericin
FBS	Fetal bovine serum
APS	Ammonium persulfate
SDS	Sodium dodecyl sulfate
TBST	Tris-buffered saline with Tween 20

TEMED	Tetramethylethylenediamine
Da	Dalton
IMAC	Immobilized metal affinity chromatography
PTP	Phosphotyrosine phosphatase
SH2	Src Homology 2
TFA	Trifluoroacetic acid
LTR	Long terminal repeats
shRNA	Short hairpin ribonucleic acid

Chapter 1: Introduction

1.1 Epidermal Growth Factor Signaling

1.1.1 Pathway and Cancer Relevance

Cell growth and proliferation processes are a normal part of the cell life cycle, which ends with cell death or apoptosis. EGF signaling is a common cell-signaling cascade that promotes cell growth and inhibits apoptosis. Elucidating the steps in this signaling pathway is a laborious process due to the sheer number of signaling components that are activated before nuclear receptors are even reached. For simplicity, the PI3K/AKT pathway is shown below to illustrate the ability of EGF signaling to inhibit apoptosis and promote cell growth.

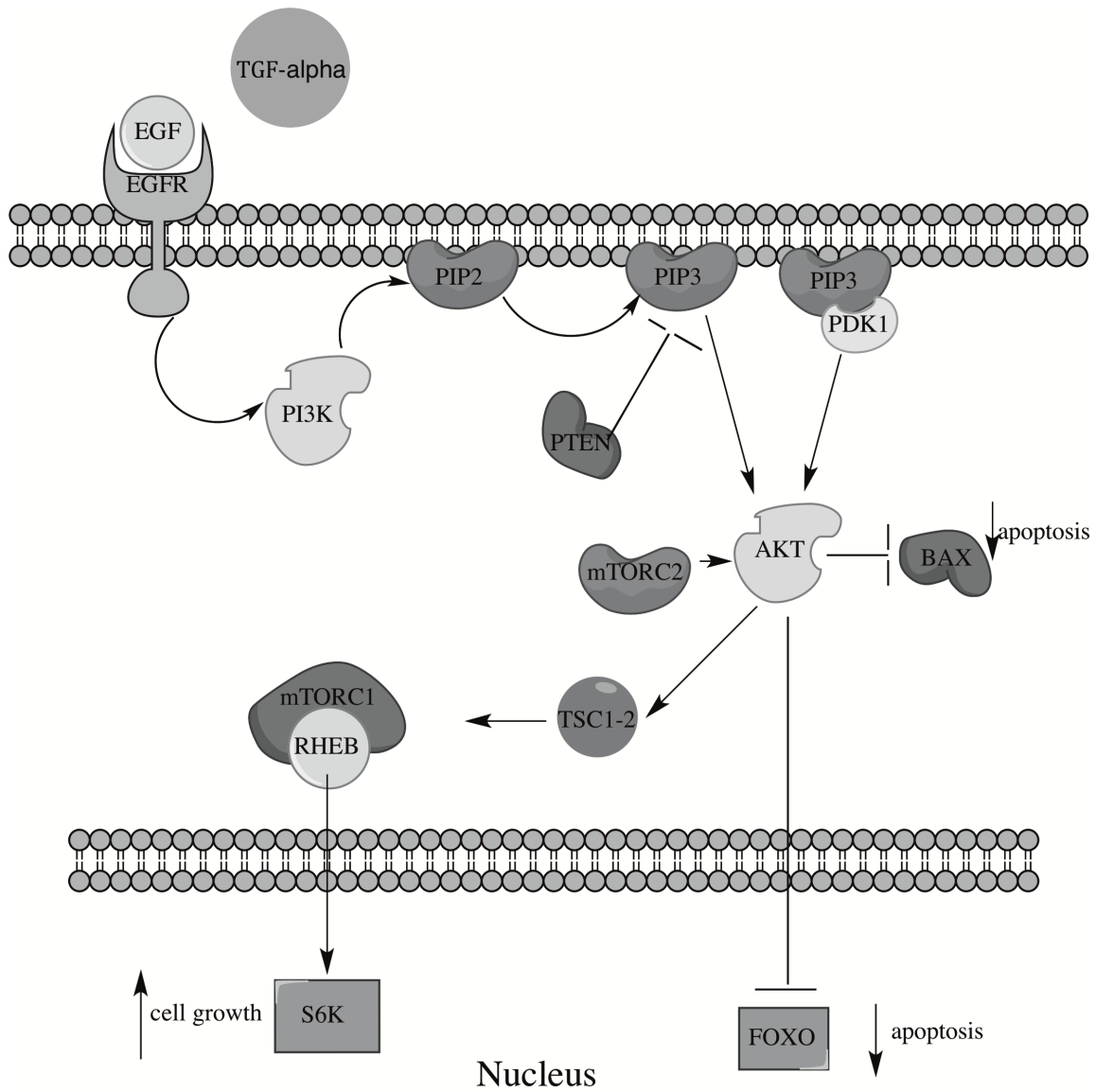


Figure 1.1 EGF signaling via the PI3K/AKT pathway. Autophosphorylation of EGFR upon EGF binding and dimerization activates the PI3K/AKT signaling pathway. Activated AKT can then inhibit BAX and/or FOXO which down-regulate apoptosis, or activate the mTOR pathway leading to cell growth.

EGF is a small 6kDa protein naturally produced by cells in the body and is part of a family of EGF proteins that also includes TGF- α .¹ These growth factors have

minimal secondary structure save for three disulfide bonds.² Both EGF and TGF- α bind cell surface tyrosine kinase receptors EGFR, ERBB2 (HER2), ERBB3 (HER3), and ERBB4 (HER4), which can then form either homo- or heterodimers.¹ All of these receptors are embedded in the cell membrane with an EGF-binding domain of two globular handles outside the cell and a tyrosine kinase enzymatic domain in the cytosol.³ The extracellular domain responsible for dimerization and the membrane embedded portion of the receptor is rigidified with many cysteine residues.³ When EGF binds, one of the cysteine-rich rods of the extracellular region is released to allow dimerization with another receptor.³ This also brings the two receptor tyrosine kinase domains in close proximity so they are able to phosphorylate one another.³ Once dimerized, and autophosphorylation occurs, the receptor tyrosine kinase domain recruits PI3K.¹ PI3K is a dimeric enzyme composed of a regulatory subunit, p85, and a catalytic subunit, p110.⁴ The regulatory subunit binds with the highest affinity for HER3 surface receptor and the catalytic subunit phosphorylates membrane-bound PIP₂ to form PIP₃.⁴ PIP₃ then recruits AKT to the cell membrane because the 120 amino acid region of AKT known as the pleckstrin homology domain has high binding affinity to PIP₃.⁵ At the same time, PDK1 interacts with another PIP₃ and AKT to phosphorylate AKT T308.⁶ To become fully functionalized, AKT is then phosphorylated at the S473 by mTORC2 away from the cell membrane.⁵ To halt phosphorylation of AKT, a tumor suppressor, PTEN dephosphorylates PIP₃ and when not properly functioning, leads to cancer in the form of glioblastomas in humans.⁷ To continue the pathway, fully activated AKT has a variety of substrates that lead to up-regulation of cell growth and proliferation and

down-regulation of tumor suppression and apoptosis. Briefly, one pathway that activates cell proliferation is the mTOR pathway where AKT inhibits TSC1-2 which releases RHEB from mTORC1.⁸ Activated mTORC1 can then signal S6K in the nucleus to promote cell growth by binding to the large subunit of ribosomes, causing them to translate mRNA into protein.⁸ Activated AKT can also prevent cell death by either binding BAX which normally creates holes in the mitochondrial membranes leading to apoptosis, or binding FOXO and phosphorylating it.^{9,10} Phosphorylated FOXO is a substrate for ubiquitin ligase, which degrades the tumor suppressor via a protease.¹⁰ This brief summary of the PI3K/AKT pathway activated by EGF stimulation does not encompass all signaling mechanisms that occur.

Now that the basic EGF signaling pathway has been elaborated on, its physiological and pathological effects can be discussed. Physiologically, EGF signaling promotes cell proliferation and survival. Therefore the main purposes of this pathway are closely linked to an organism's development into adulthood and cell turnover including wound healing. Studies on both the over stimulation with EGF and over expression of EGFR coupled with EGFR knockouts have proven that a balance of signaling is essential for proper development in embryonic mice.¹¹ Knockout mice in particular showed severe growth inhibition and multiple organ failure before reaching maturity with the worst-case scenario as mid-gestational death.¹¹ If they survive birth, the mice show severe abnormalities in skin, lungs, the gastrointestinal tract, brain, and liver highlighting the breadth of influence EGFR carries.¹¹ However if TGF α -null mice are observed, the phenotype is wavy fur and whiskers implying it's importance as a signaling molecule in the epidermis but also

showing that other signaling peptides are able to compensate and prevent severe deformity.¹² Since EGFR is one of four homologues that can form homo- and heterodimers in the ErbB family, each combination with a preference for different signaling peptides like EGF, it comes as little surprise that when knocking out receptors or ligands, there is some compensation in signaling. Overexpression of EGFR caused mice to spontaneously grow tumors.¹² One particular mouse model expressed a common mutation to the EGFR called EGFRvIII where exons 2-7 are deleted yielding a protein that lacks the majority of the extracellular domain.¹³⁻¹⁴ The cell interprets this as a constantly activated receptor and thus this mutation is seen in 40-50% of grade VI glioblastomas and in up to 70% of medulloblastomas with a small proportion of breast and ovarian carcinomas.¹⁵⁻¹⁶ Interestingly the overexpression of signaling ligand TGF α does show increased cell proliferation but mainly in the form of psoriasis and development of papillomas at the site of a wound without progression to carcinomas.¹⁷⁻¹⁸ Clearly the relationship between EGF ligand and EGFR binding can have a varied effect on cell proliferation and cancer pathology, making it a hot target for the development of anti-cancer drugs and therapies.

With so many components to the EGF signaling pathway, each becomes a potentially druggable target. The first druggable target is EGFR, which has two major drug types on the market currently: tyrosine kinase small molecule inhibitors and monoclonal antibody therapies. Popular tyrosine kinase inhibitors include gefitinib (Iressa) and erlotinib (Tarceva), which target the ATP binding site, K745, in the tyrosine kinase region of EGFR.¹⁹ Resistance to these drugs is the

responsibility of mutations near this binding site including T790M and L858R, which has mainly been studied in NSCLC, the leading cause of cancer death in the United States.¹⁹⁻²⁰ Monoclonal antibody therapies include cetuximab (Erbix) and panitumumab (Vectibix), which targets the ligand binding domains of untethered EGFR so that it cannot be activated.²¹ These therapies are mostly limited by differences between ErbB family members.²¹ The next potential target for anti-cancer therapies is PI3K. Idelalisib is a small molecule ATP binding inhibitor that targets the p110 δ (one of four isoforms of p110) subunit of PI3K.²² Other small molecule inhibitors that specifically target the PI3K ATP binding pocket include Wortmannin, LY294002, Quercetin, Myricetin, and Staurosporin which all have multi-ring structures.²³ Of these, all are reversible inhibitors except for Wortmannin, which forms a covalent bond with K833.²³ Another potential target in the EGF signaling pathway is tumor suppressor PTEN. Restoring activity to PTEN or other tumor suppressors in systems where they have lost function has proven more difficult than targeting oncogenes and components that have a gain of function.²⁴ Therefore as an example of a therapy involving PTEN, an ErbB2-targeting antibody, trastuzumab (Herceptin) has been explored.²⁵ Nagata et. al. were able to demonstrate that treatment with trastuzumab caused PTEN to localize at the cell membrane and activate its phosphatase activity by reducing PTEN tyrosine phosphorylation.²⁵ For patients with PTEN-deficient breast cancers it was shown to resist treatment with trastuzumab.²⁵ The next major component of the EGF signaling pathway, AKT, has a much larger pool of therapies for treatment of excess cell growth and proliferation. In particular, an allosteric inhibitor, MK-2206, has

been shown to enhance the efficacy of cancer treatment cocktails including treatment with erlotinib or LY294002.²⁶ Another inhibitor, Afuresertib, is a reversible ATP competitive inhibitor for AKT.²⁷ It is currently in phase IIa clinical trials and has shown tolerable side effects for patients suffering a rare disease, Langerhans cell histiocytosis.²⁷ Other inhibitors of AKT include GSK690693, AKT inhibitor VIII, and AKT inhibitor IV, which do not have any structural relevance but all cause a decrease in cell viability and apoptosis by out-competing ATP.²⁸ The last major marker of the EGF signaling pathway is mTOR. When discussing therapies for targeting mTOR, they most likely refer to the targeting of mTOR1 specifically since mTOR2 is not specific to rapamycin and selective inhibition has been elusive.²⁹ Two molecules, pyrazolopyrimidines, that specifically target mTOR are PP242 and PP30 and work as ATP-competitive inhibitors to prevent phosphorylation of S473 on AKT.²⁹ Although rapamycin, also termed Rapamune or sirolimus, has been used for a longer period of time to target mTOR and reduce cell proliferation, these inhibitors show stronger efficacy in preliminary studies.²⁹ Other drugs, temsirolimus (Torisel) and everolimus (Afinitor), are used to target mTOR by forming a complex with an abundant intercellular protein, FKBP-12, that then complexes with mTOR to deactivate it.³⁰⁻³¹ From all of the various drugs listed, the EGF signaling pathway has clearly been a considerable target of interest for cancer therapies. Limitations usually appear in the form of binding specificity and ability to permeate the cell membrane without causing intolerable side effects. However, factors besides protein phosphorylation play major roles in cell signaling and cancer cell growth including ROS.

1.1.2 Production of Reactive Oxygen Species

EGF signaling is known to produce ROS in the form of hydrogen peroxide and basal levels of ROS in the low-nanomolar to low-micromolar range act as signaling molecules.³²⁻³⁴ However, if overproduced, ROS can have destructive oxidative effects on many cellular components leading to cell proliferation associated with cancer.³² ROS is a broad term used to encompass a variety of oxidative species including singlet oxygen ($^1\text{O}_2$), superoxide anion radical ($\text{O}_2^{\bullet-}$), hydrogen peroxide (H_2O_2), and hydroxyl radical (OH^{\bullet}).³² As described previously, EGF binds EGFR and through phosphorylation signaling, activates PI3K.¹ PI3K then phosphorylates PIP_2 to PIP_3 , which then activates the AKT signaling pathway.

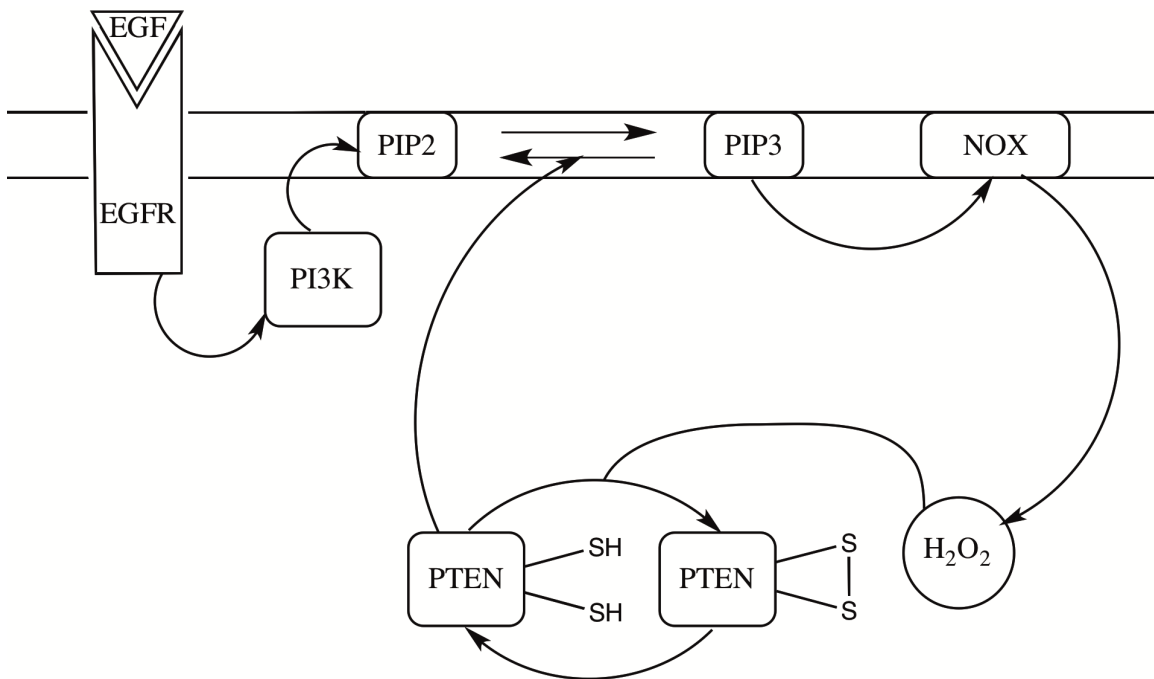


Figure 1.2 Production of hydrogen peroxide as it relates to EGF signaling.

Activation of the PI3K/AKT pathway not only down-regulates apoptosis and up-regulates cell growth but can also produce hydrogen peroxide ROS when PIP_3 activates NOX. Hydrogen peroxide can inhibit PTEN by oxidizing cysteine residues

to form a disulfide bond, allowing PIP₃ to remain activated and promoting activation of the PI3K/AKT pathway.

PIP₃ also activates NADPH oxidase, NOX1, complex, as shown above, which enzymatically removes electrons from NADPH and reduces oxygen at the cellular membrane to give superoxide anions.³⁵ This generation of ROS is extracellular and although many believe hydrogen peroxide simply diffuses across the membrane, mounting evidence shows that a nearby aquaporin channel translocation is preferred.³⁶⁻³⁸ Once in the cell, these ROS can be reduced to molecular oxygen and hydrogen peroxide via superoxide dismutases whose cellular function is to reduce harmful ROS in cells.³⁹ The hydrogen peroxide product can then oxidize various cellular components, however due to proximity, the PIP₃ deactivator and tumor suppressor PTEN is a more likely target.³⁵ The catalytically active cysteine residue C124, which normally dephosphorylates PIP₃, is oxidized and forms a disulfide bond with C71 on the protein.⁴⁰ This reversible oxidation cycle is completed when Trx reduces PTEN, exposing the free thiols so that C124 can dephosphorylate PIP₃.³⁵ Dephosphorylation by catalytic cysteine residues is common among PTP family members including PTEN because the pK_a of the active site cysteine is much lower than the average free thiol (pK_a=4-6.5).⁴¹ This allows the generation of a cysteinyl phosphate intermediate within the enzyme that is then hydrolyzed.⁴¹ This enzymatic process highlights cysteine sensitivity to protein microenvironments and redox chemistry upon ROS generation.

Basal levels of ROS are a vital part of cell signaling. To avoid the consequences of overproduction as previously described, intracellular species are used as buffers to reduce and eliminate ROS. Common ROS buffer systems include Trx and Prx with a lesser contribution from GSH:GSSG.³³ Trx has been shown to undergo significant oxidation upon ROS generation in response to EGF signaling and Prx can efficiently eliminate hydrogen peroxide at a rate constant of 10^5 - 10^8 $M^{-1}s^{-1}$.⁴²⁻⁴³ GSH, although abundant at millimolar concentrations, is too slow at reducing ROS to be considered effective.⁴⁴ ROS derived cell signaling at these basal levels range the EGF signaling pathway as previously described and provide a system of checks and balances to maintain normal cell function.

1.2 Role of Cysteine as it Relates to Reactive Oxygen Species

1.2.1 Cysteine Oxidation and Disulfide Bond Formation

Cysteine is one of the least abundant amino acids but is usually found in functionally important locations due to the free thiol side chain. The free thiol $pK_a=8-9$ and is closest to physiological pH (7.4) giving rise to high sensitivity to minute changes in the protein environment.⁴⁵ For comparison, the next closest pK_a to physiological pH is $pK_a=6.0$ for histidine side chains. Since the thiol group has a larger atomic radius and lower dissociation energy between the S-H bond, it can participate in both nucleophilic and redox chemistry. Free thiols can be oxidized multiple times via ROS: reversibly to form either a disulfide bond or sulfenic acid, but irreversibly to form either sulfinic or sulfonic acid.

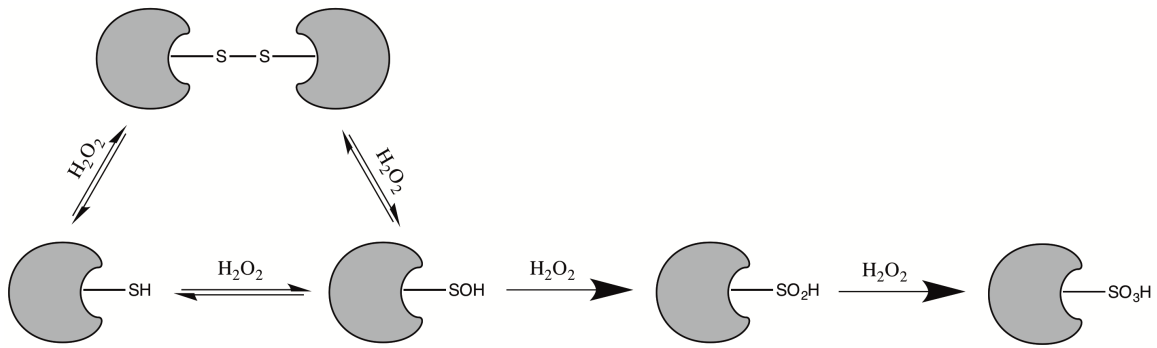


Figure 1.3 Oxidative PTMs of cysteine residues. The cysteine free thiol (S^{-2}) can be oxidized to form either a disulfide bond (S^{-1}) or sulfenic acid (S^0) reversibly. The disulfide bond can also be reversibly oxidized to form sulfenic acid. Sulfenic acid can then be irreversibly oxidized to sulfinic acid (S^{+2}), which can further be irreversibly oxidized to sulfonic acid (S^{+4}).

Other post-translational modifications include nitrosylation and glutathionylation.⁴⁵ With these unique properties, cysteine residues play a variety of cellular roles: they can bind metal ions and make up the iron-sulfur clusters in ferredoxins, act as catalytic nucleophiles in caspases, adopt regulatory roles in kinases such as the EGFR, form structural disulfides seen in keratin, and act as redox catalytic sites for PTEN.⁴⁶⁻⁵⁰ Two significant examples of ROS effects on cysteine residues as it relates to EGF signaling are the oxidation of EGFR and AKT. In the ATP-binding pocket of EGFR, C797 has been shown to undergo modification due to ROS generated by EGF signaling.³³ Carroll et. al. has demonstrated that upon EGF addition, oxidation of C797 to form the sulfenylated product, increased EGFR kinase activity by approximately five-fold.³³ This residue, interestingly, is conserved

within nine other receptor and non-receptor tyrosine kinases and leads to an increase in downstream signaling.^{33, 51} Another major component of the EGF signaling pathway, AKT, has been shown to undergo sulfenic acid modification at C124 to inactivate the kinase.⁵² To protect C124 from ROS-induced oxidation, researchers have shown that an overexpression of Grx sustains AKT phosphorylation.⁵³ The adverse roles cysteine can perform make this residue a target for studying protein function and disease related to cysteine mutation and modification.

1.2.2 Monitoring Cysteine Reactivity in Living Cells

One way to effectively monitor cysteine reactivity and modification is by exploiting its nucleophilicity. Iodoacetamide alkyne is highly electrophilic probe that has shown great utility when used to monitor cysteine reactivity within a proteome.⁵⁴ In proteomics experiments, after treating cell lysate with IA-alkyne, copper(I)-catalyzed azide-alkyne cycloaddition can be used to incorporate a reporter group which can be a fluorescent tag such as Rhodamine azide for in-gel fluorescence experiments, or isotopically labeled azo tags developed for quantitative mass spec analysis.⁵⁴

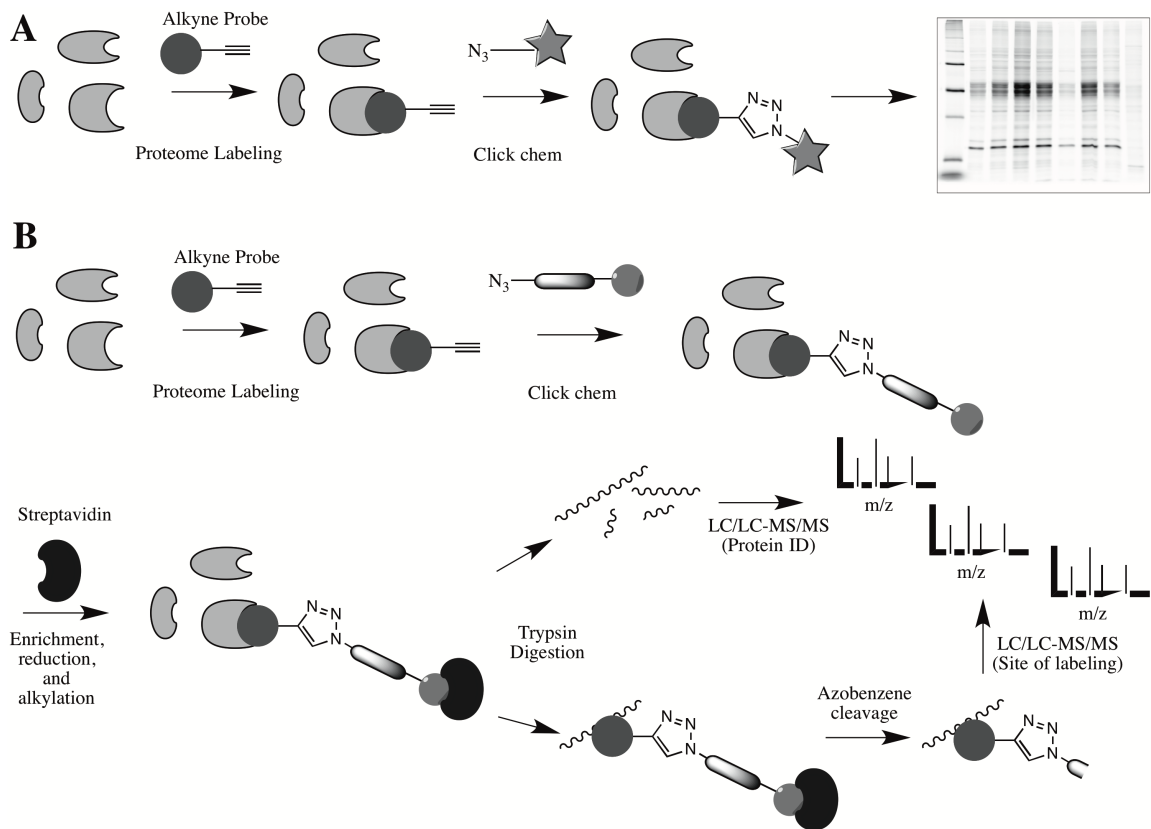


Figure 1.4 Use of Iodoacetamide alkyne to probe the proteome analyzed by in-gel fluorescence and mass spectrometric methods (adapted from Weerapana et. al., 55). Iodoacetamide alkyne specifically labels cysteine residues available throughout the proteome. The alkyne handle is then available for click chemistry with either a fluorescent tag that can be used to monitor in-gel fluorescence (A) or a biotinylated tag that can be used to isolate tagged proteins via streptavidin bead enrichment (B). The isolated proteins can then be digested with trypsin for peptide analysis and the tag can be cleaved for site of labeling analysis via mass spectrometry.

However since cysteine reactivity is highly influenced by the protein microenvironment, more accurate data would be obtained if labeling could occur in

living cells and although IA-alkyne is cell-permeable, it is cytotoxic.⁵⁶ Therefore a α -bromomethyl ketone electrophile was developed by Dr. Masahiro Abo of the Weerapana lab.⁵⁶

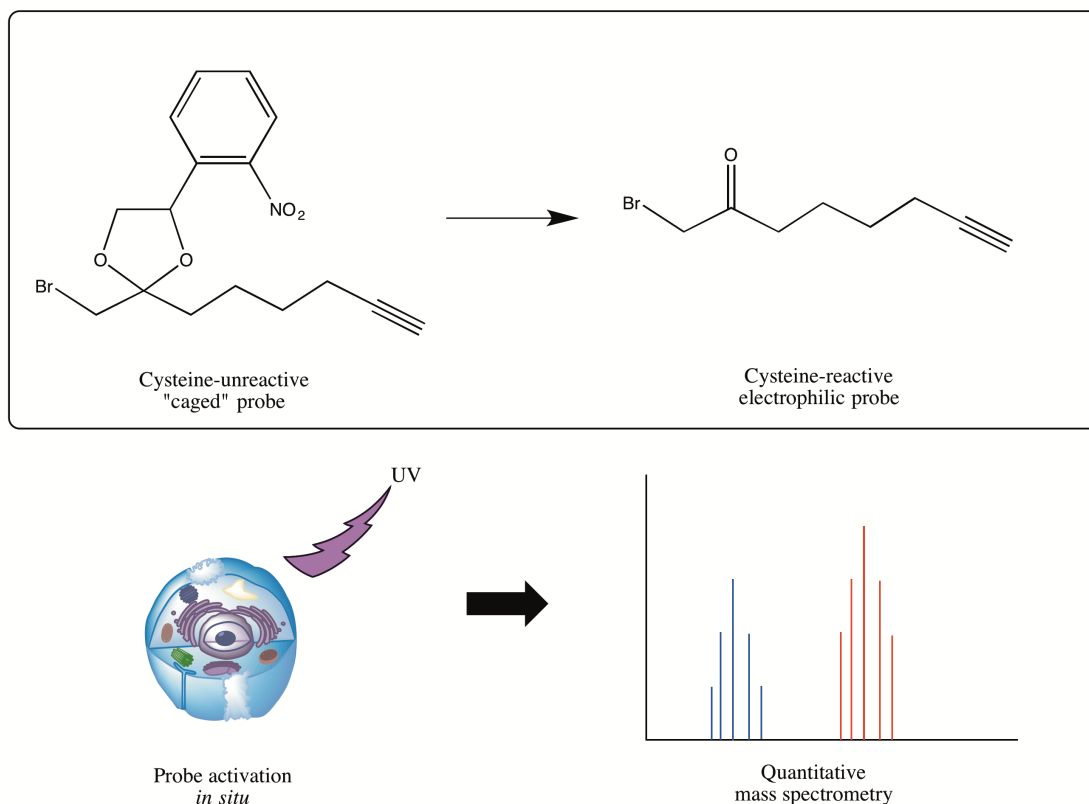


Figure 1.5 Caged electrophile for live cell labeling and analysis via mass spectrometry (adapted from Abo et. al., 56). On the top the structure of the caged probe and uncaged electrophile are shown. The bottom images show that once irradiated with UV light, cells can be harvested, lysed, and prepared for analysis via mass spec.

His probe is a caged electrophile that can accumulate in cells without cytotoxic effects up to 500 μ M.⁵⁶ To label proteins once cells have been treated with the

caged-BK probe, they are irradiated with UV light to uncage the probe and expose the BK electrophile.⁵⁶ Cells can then be harvested, lysed, and subjected to CuACC for in-gel fluorescence or mass spec analysis.⁵⁶ Once the caged-BK labeling protocol was optimized, A431 cells were used to observe cysteine reactivity upon EGF stimulation due to their overexpression of EGFR.⁵⁶ This experiment gave information about the oxidative modifications on cysteine from physiological production of ROS. The major findings were that upon EGF stimulation, a large number of cysteines decreased reactivity when compared to the control sample without EGF stimulation.⁵⁶

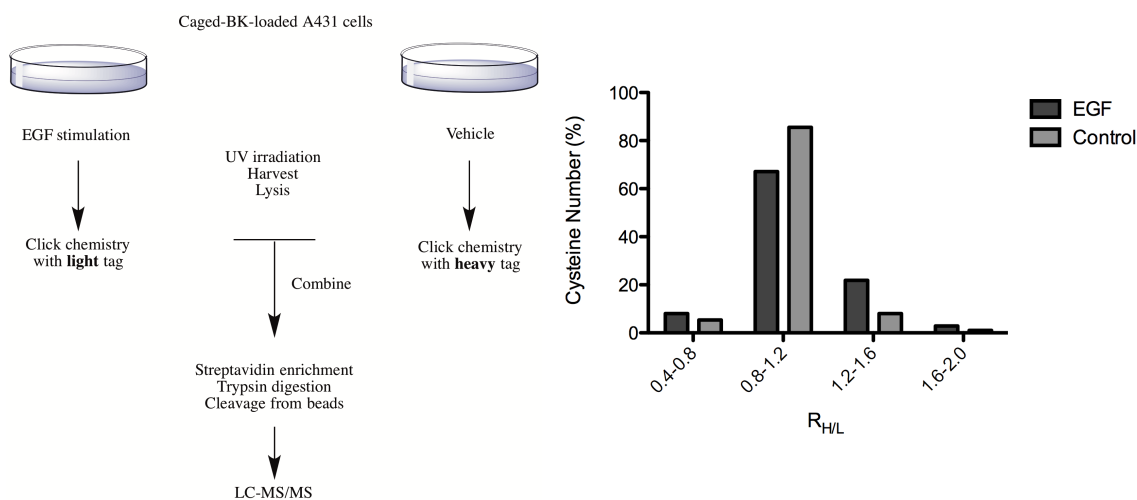


Figure 1.6 Results comparing cysteine oxidation in cells with and without EGF stimulation (adapted from Abo et. al., 56). Left: sample preparation work-flow leading to LC-MS/MS analysis. Right: the number of cysteine residues labeled for the control and EGF samples in a particular $R_{H/L}$ range. The heavy to light ratio

(R_{H/L}) shows that upon EGF stimulation, cysteine oxidation causes a loss of labeling in the overall proteome therefore increasing the ratio for treated cells.

This result should be anticipated since EGF stimulation is known to increase ROS production and therefore more cysteine residues should be oxidized. Many of the cysteines modified were known to form redox-active disulfide bonds or become S-sulfenylated thus confirming the utility of this probe.⁵⁶ One of the proteins showing the largest shift was FABP5 with emphasis on the C120 residue.⁵⁶ Since most studies involving FABP5 have focused on other binding site residues with minimal attention given to the potential disulfide bond between C120 and C127, we decided to investigate their role in EGF signaling further.

1.3 Fatty Acid Binding Protein 5

1.3.1 Fatty Acid Binding Protein Family

The FABP family, or iLBP family, consists of ten members: liver (L-, 1), heart (H-, 3), adipocyte (A-, 4), epidermal (E-, 5), ileal (I-, 2), brain (B-, 7), myelin (M-, 8), gastrophin and ileal (Il-, 6), testis (T-, 9) and FABP12.⁵⁷⁻⁵⁸

```

FABP2      ----MAFDSTWKVDRSENYDKFMEKMGVNIIVKRKLAHDNLKLTITQEGNKFTVKES-SA
FABP5      MATVQQLEGRWRLVDSKGFDEYMKELGVGIALRKMAMAKPDCIITCDGKNLTIKTE-ST
FABP3      --MVDAFLGTWKLVDKSNFDDYMKSLGVGFATRQVASMTKPTTIIKNGDILTLLKTH-ST
FABP7      --MVEAFCATWKLTSQNFDEYMKALGVGFATRQVGNVTKPTVIIISQEGDKVVIRTL-ST
FABP12     --MIDQLQGTWKSISCESEDYMKELGIGRASRKLGRRLAKPTVTISTDGDVITIKTK-SI
FABP4      --MCDAFVGTWKLVSSENFDDYMKELGVGFATRQVAGMAKPNMIISVNGDVITIKSE-ST
FABP9      --MVEPFLGTWKLVSSENFEDYMKELGVNFAARNMAGLVKPTVTISVDGKMMTIRTE-SS
FABP8      --MSNKFLGTWKLVSSENFDDYMKALGVGLATRKLGNLAKPTVIIISKKGDIITIRTE-ST
FABP1      ----MSFSGKYQLQSQENFEAFMKAIGLPEELIQKGDIKGVSEIVQNGKHFKFTIT-AG
FABP6      ----MAFTGKFEMESEKKNYDEFMKLLGISSDVIEKARNFKIVTEVQQDQDFTWSQHYSG
           : . : . : . : * : * : : . : : : * . . :

FABP2      FRNIEVVFELGVTFNYNLADGTELRGTWSLEGN-KLIGKFKRTDNGNELNTVREIIGDEL
FABP5      LKTTFQFCTLGEKFEETTADGRKTQTVCNFTDG-ALVQHQE--WDGKESTITRKLKDGKL
FABP3      FKNTEISFKLGVFEDETTADDRKVKSIIVTLDDGG-KLVHLQK--WDGQETTLVRELIDGKL
FABP7      FKNTEISFQLGEEFDETTADDRNCKSVVSLDGD-KLVHIQK--WDGKETNFVREIKDGKM
FABP12     FKNNEISFKLGEFEETTPGGHKTKSKVTLDE-SLIQVQD--WDGKETITRKLVDGKM
FABP4      FKNTEISFILGQEFDEVTADDRKVKSTITLDGG-VLVHVQK--WDGKSTTIKRKREDDKL
FABP9      FQDTKISFKLGEFEDETTADNRKVKSTITLENG-SMIHVQK--WLGKETTIKRKIVDEKM
FABP8      FKNTEISFKLGEFEETTADNRKTKSIVTLQRG-SLNQVQR--WDGKETTIKRKLNVGKM
FABP1      SKVIQNEFTVGECELETMTGEKVKTVVQLEGDNKLVTTFK-----NIKSVTELNGDII
FABP6      GHTMTNKFVVGKESNIQTMGGKTFKATVQMEGG-KLVVNFPP-----NYHQTSEIVGDKL
           : : * : . : : : : . : . :

FABP2      VQTYVYEGVEAKRIFKKD-----
FABP5      VVECVMNNVTCTRIYEKVE-----
FABP3      LLTLTHGTAVCTRTYEKEA-----
FABP7      VMTLTFGDVVAVRHYEKA-----
FABP12     VVESTVNSVICRTRTYEKVSSNSVSNS
FABP4      VVECVMKGVTSRVIYERA-----
FABP9      VVECKMNNIVSTRYIEKV-----
FABP8      VAECKMKGVVCTRIYIEKV-----
FABP1      TNTMTLGDIVFKRISKRI-----
FABP6      VEVSTIGGVTYERVSKRLA-----
           * : :

```

Figure 1.7 Sequence homology between FABP family members. FABP family members' sequences were taken from UniProt database and aligned via Clustal Omega. The notation below specific residues indicates how conserved they are. A single dot shows that a specific amino acid occurs relatively frequently in that position, a double dot shows that the amino acid occurs in almost all family members at that position, and a star denotes that a specific amino acid is conserved among all family members.

Although their sequence similarity ranges from 38-70%, three structural defining features are conserved throughout the family: the β -clam structure with five anti-parallel β -strands on each side, an α -helical lid, and a hydrophobic binding pocket for fatty acids and lipids.⁵⁸⁻⁵⁹ Ligands are typically bound in a 1:1 ratio with the exception of L-FABP, which is able to bind two fatty acids simultaneously.⁵⁸ Typical substrates include but are not limited to palmitic, stearic, oleic, arachidonic, and linoleic acids, lysophospholipids, eicosanoids, and retinoids.⁵⁷ The sequence variety distinguishes each FABP's function and ligand specificity. Unique to FABP5 are its cysteine residues. There are six total throughout the protein including C43, C47, C67, and C87 which are completely unique and C120 and C127 which are both also found in M-FABP, but only one of the two cysteines in the binding pocket are found in other FABP family members.⁶⁰ The only FABP with a proposed disulfide bond is FABP5 between C120 and C127. Technically C67 and C87 are close together in the crystal structure of FABP5 however after crystal structure refinement, the electron density map indicated that a disulfide bridge was not present and when one was superimposed, the model protein did not match the electron density map.⁶⁰⁻⁶¹ Although M-FABP has two cysteine residues in the binding pocket and despite biochemical evidence, a disulfide bond isn't thought to exist based on the S-S distance from X-ray structure analysis.⁶² The other binding pocket residues in FABP5, R109, R129, and Y131 are relatively well conserved throughout the iLBP family with R129 found in all members and R109 and Y131 found in most members.⁵⁷ Other residues of functional interest, including the nuclear localization signal residues, are well conserved however the activating switches of FABP5 (M35

and L60) are unique to that protein.⁵⁷ Deviations in the activating switch regions account for the different ligand binding profiles for each member of the iLBP family.

FABPs constitute 1-5% of all cytosolic proteins and the expression of a particular FABP is not limited to one specific cell type.⁶³ The protein expression levels are indicative of the relative amount of fatty acid present and lipid metabolism each cell type is involved in.⁵⁷ Therefore with such divergence between expression and ligand binding, it should come as no surprise that a multitude of cellular functions has been proposed for this family of proteins. Most proposals center on the theory that the roles of FABPs are to 1) solubilize hydrophobic molecules, 2) shuttle ligands to their appropriate location in the cell, and 3) protect their substrates from peroxidation.^{57, 64} One of the best-studied roles of FABPs is their nuclear transport of fatty acids to the PPAR nuclear transcription factors, which regulate transcription of multiple FABPs leading towards cell survival and proliferation in cancer as described previously. Other diseases implicated in FABP associated pathways include psoriasis, diabetes, obesity, and atherosclerosis.⁵⁸ The incredibly varied ligand binding profile of FABPs has made the development of drugs difficult. Many current small molecule drugs under investigation are modeled after or compared to small-molecule inhibitor BMS309403, derived from different carbazole- and indole- inhibitors, which bind A-FABP with high affinity and selectivity over other FABPs to treat atherosclerotic lesions.⁶⁵⁻⁶⁷ Given the difficulties of designing effective drugs with high affinity for specific FABPs, knowledge regarding the contributions of all residues within the FABP binding pocket is essential for the development of inhibitors to treat disease.

1.3.2 Cellular Function and Cancer Relevance

FABP5 was originally discovered in keratinocytes of psoriasis patients; a disease characterized by rapid cell turnover and disordered lipid metabolism.⁶⁸ It is mainly expressed in epidermal cells of the skin but is also expressed in tongue, adipose tissue, dendritic cell, mammary gland, brain, kidney, liver, lung, and testis tissues.⁶⁹⁻⁷¹ Ligands commonly bound include a wide variety of saturated and unsaturated fatty acids including stearic, linoleic, palmitic, oleic, arachidonic, eicosapentanoic, and docosahexaenoic acid, however only those that can adopt a U-shape versus L-shape conformation activate the protein for nuclear translocation.⁷²⁻⁷³ FABP5 can also bind other lipophilic compounds including retinoic acid, which has been linked to cancer via the activation of the PPAR pathway.

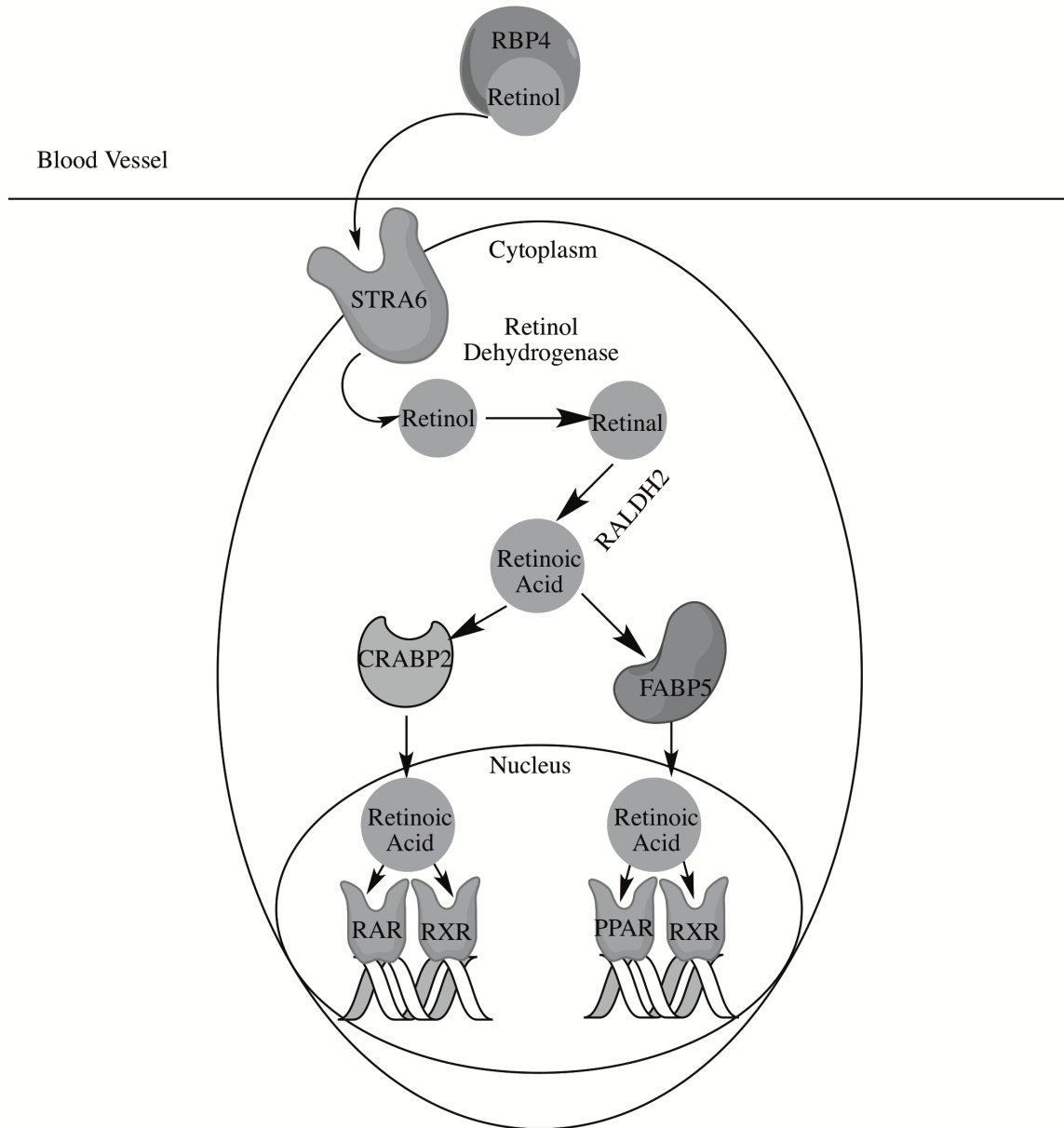


Figure 1.8 Relevance of FABP5 in retinoic acid signaling pathway (adapted from van de Pavert et. al., 74). Retinol from the blood stream is transported into cell cytoplasm via STRA6 where it is converted into retinoic acid. Retinoic acid can then be taken to the nucleus by either CRABP2, which delivers it to signal nuclear receptors RAR and RXR causing growth inhibition, or FABP5, which signals

nuclear receptors PPAR β and RXR to stimulate a positive feedback loop for cell growth.

Retinol, or vitamin A, is obtained from dietary intake and stored in the liver.⁷⁴ There, it complexes with RBP4 which can be taken up by cells via STRA6.⁷⁴ Once in the cytoplasm, retinol is converted to retinal via retinol dehydrogenase then to retinoic acid by RALDH2.⁷⁴ Following the retinoic acid pathway, either FABP5 or CRABP-II binds the substrate and transports it to the nucleus.⁷⁴ FABP5 specifically interacts with nuclear receptor PPAR β which controls keratinocyte differentiation, counteracts the apoptotic role of TNF- α , and upregulates the expression of FABP, VEGF, and PDK1, creating a positive feedback loop.⁷⁵⁻⁷⁶ CRABP-II specifically interacts with RAR, which promotes growth inhibition.⁷⁷ Note that both PPAR β and RAR must form a heterodimer with RXR to be able to bind promoter regions and activate transcription.⁷⁶ In normally functioning cells, CRABP-II and FABP5 are expressed such that the relative ratio of CRABP-II:FABP5 is above one.⁷⁷ Combined with a stronger binding affinity for the CRABP-II-RA-RAR complex than the FABP5-RA-PPAR β complex and free fatty acids outcompeting RA, rampant cell proliferation is kept in check.⁷⁷⁻⁷⁸ In cases of higher-grade tumors taken from ER-negative breast cancer patients, FABP5 is upregulated, causing resistance to retinoic acid therapy and poorer prognosis.⁷⁷ FABP5 is upregulated when EGF activates NF- κ B through the PI3K/AKT pathway as described previously.⁷⁷ Since the major function of fatty acid binding proteins relates to metabolism there are carcinogenic implications with the misregulation of all members of the FABP family.⁷⁹

1.3.3 Binding Pocket and the Relevance of Cysteine Residues

FABP5 (also known as E-FABP, PA-FABP, C-FABP, K-FABP, or mal1) is a 15kDa cytosolic protein that transports long chain fatty acids to the nucleus for cellular signaling.^{72, 80}

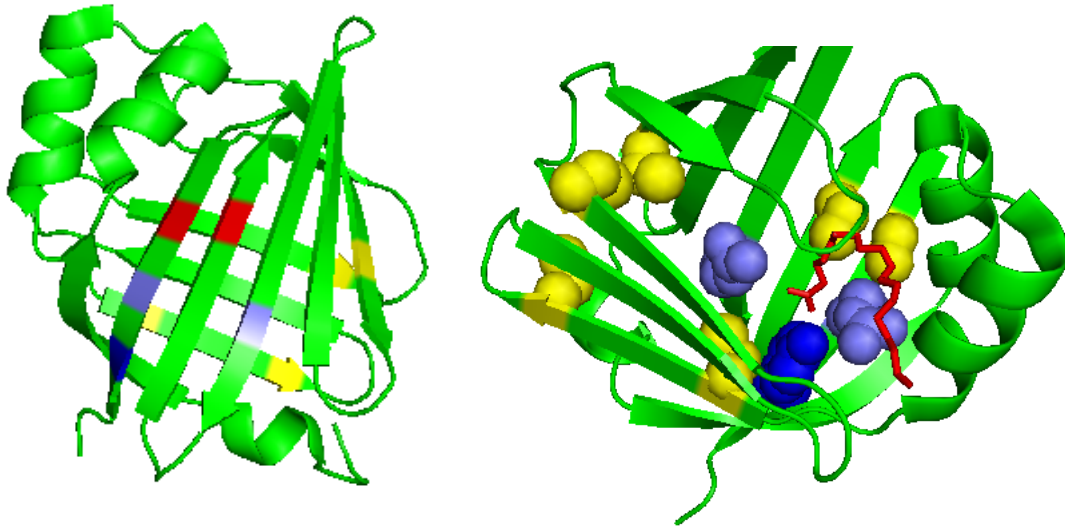


Figure 1.9 Crystal structure of FABP5 bound to linoleic acid (PDB: 4LKT).

The left image shows the entire structure of FABP5 with binding site residues R109 and R129 in light blue and Y131 in dark blue, C120 and C127 in red, and the remaining cysteine residues in yellow. The right image shows FABP5 from the perspective of looking into the binding pocket from the entryway made by the α -helical lid where R109 and R129 in light blue, Y131 in dark blue, all cysteine residues in yellow, and bound linoleic acid in red. The two cysteine residues overlapped in this image by the bound fatty acid are C120 and C127 from left to right respectively.

The protein has a highly conserved β -clam structure with two orthogonal β -sheets with five anti-parallel β -strands each. There is also an α -helical lid with a helix-turn-helix motif, which encloses the bound fatty acid during nuclear transport.⁶¹ Although FABP5 can bind a variety of saturated and unsaturated fatty acids, those that are polyunsaturated and have the ability to adopt more of a U-shape conformation disrupt the β 2 portal loop.⁷² Disruption of the portal loop causes the α -helical lid to enclose the fatty acid and expose the nuclear localization signal region of the protein made up of residues K24, K34, and R33.⁷² Long chain fatty acids that bind FABP5 but have a more L-shape configuration are not fully enclosed within the binding pocket with the fatty acid tail exposed to solvent at the portal loop region.⁷² This prevents interaction between the M35 residue of the α 2 helix and L60 residue of the β 2 loop, which act as the “activating switches” for nuclear transport.⁷² The interior of the protein is lined with hydrophobic side chains that stabilize the fatty acid alkyl tail via van der Waals forces and a binding site composed of R109, R129, and Y131 which interact with the carboxylic head group. The strongest interaction is the salt bridge formed with R129 with hydrogen bonding to the other binding site residues.⁷² Interestingly two cysteine residues are located close to the binding site with C120 near the gamma carbon of the fatty acid alkyl chain. Previous crystallographic studies have determined that these two cysteine residues are close enough for disulfide bond formation. The most recent findings from X-ray crystallography indicate that when a fatty acid is bound, the potential disulfide bond is reduced and in apoprotein there is a mixture of disulfide bound and sulfhydryl forms of the cysteine residues.⁷² Mass spectrometry studies have also provided

evidence that these residues may form a disulfide bond through S-sulphenylation studies. Yang et. al. showed that upon treatment with H₂O₂, C127 was more sulphenated than C120 suggesting that S-sulphenylation of C127 was responsible for disulfide bond formation.⁸¹ Otherwise, few studies have focused on the biological relevance of these cysteine residues and their effects on FABP5's activity.

1.4 Experimental Goals

Given the functional relevance of cysteine residues and their location in the binding pocket of FABP5, our aims for this project are to characterize the role of C120 and probe the role of disulfide bond formation in FABP5 within the context of EGF signaling. In order to characterize the C120 residue, WT FABP5 along with the following mutants: C120S, C127S, C120/127S, and R109A will be recombinantly expressed in *E. coli*. Fluorescence assays will then be optimized to monitor cysteine reactivity under various conditions including oxidation and reduction via GSH/GSSG and in the presence of palmitic acid. We then propose to transfect A431 human cells to either over express or knock out FABP5. This will allow us to observe phenotypic characteristics and allow for studies using western blot and phosphoproteomic techniques to understand the role of FABP5 upon EGF stimulation.

Chapter 2: Experiments and Results

2.1 Recombinant Expression of WT and Mutant FABP5

WT FABP5 was first cloned into a pET-DUET vector in BL21 cells. Next, the mutants C120S, C127S, and C120/127S were made and also expressed in BL21 cells. All proteins were then overexpressed with IPTG induction and purified using nickel columns (to remove all other proteins), PD10 columns (to remove the excess imidazole salt), and then hydroxyalkoxypropyl dextran columns (to remove any bound fatty acids to FABP5) as shown in Figure 2.1.

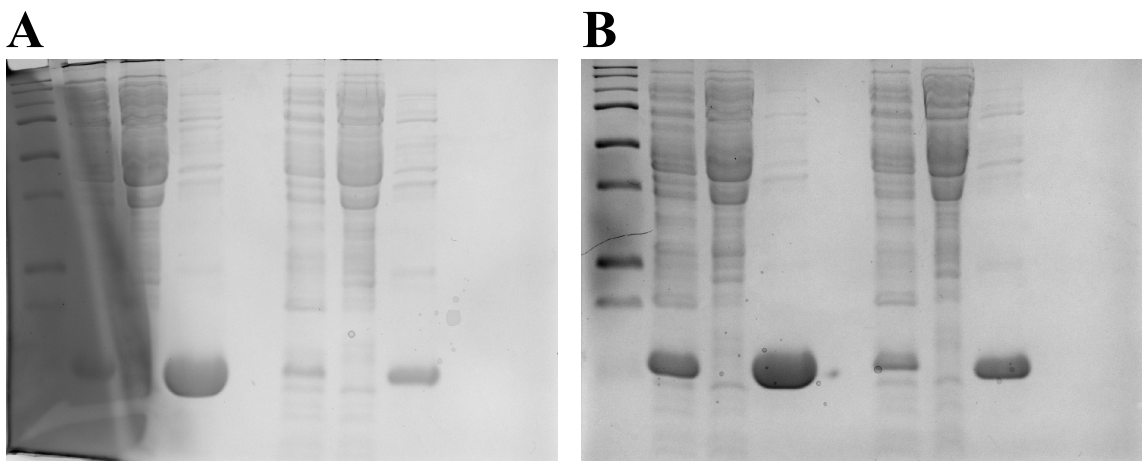


Figure 2.1 Coomassie images of the purification of WT and all mutant FABP5

overexpression large-scale growths. The order of gel A (from left to right) is: Protein ladder (R), WT protein lysate, WT protein after 25mM imidazole wash on a Ni column, WT protein final purified sample after using a PD10 column and hydroxyalkoxypropyl dextran column, empty lane, C120S protein lysate, C120S protein after 25mM imidazole wash on a Ni column, and C120S protein final purified sample after using a PD10 column and hydroxyalkoxypropyl dextran column followed by empty lanes (saved as 05052016gel1). The order of gel B (from left to right) reflects the same steps in the

purification process as gel A, however after the lane with protein ladder (R), the order of protein is C127S then C120/127S (saved as 05052016gel2).

Once all proteins were confirmed to overexpress and purify successfully, Figure 2.2 was used to show that clean purification was possible for each FABP5 variant and that a Bradford assay was sufficient to determine protein concentration.

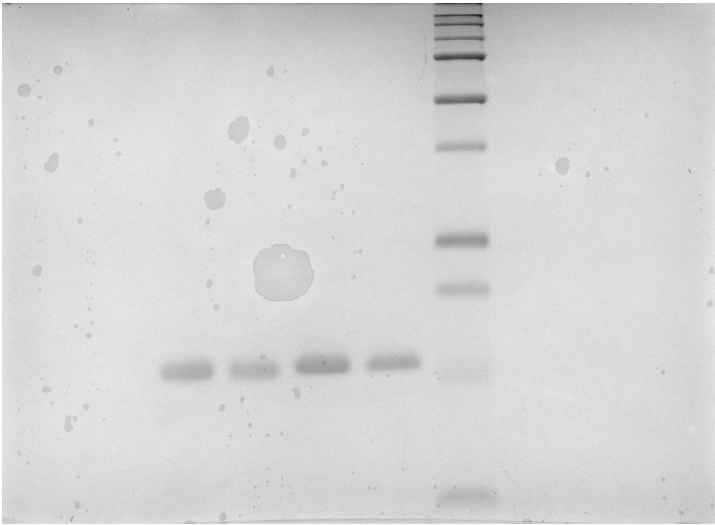


Figure 2.2 Coomassie image of purified WT and all mutant FABP5. The order of the gel (from left to right) is blank lanes, protein fluorescent ladder (F) (which should not appear with any bands), WT FABP5, C120S FABP5, C127S FABP5, C120/127S FABP5, protein ladder (R), and more blank lanes (saved as 02112016).

The next step was to determine the appropriate fluorophore to use in the fluorescence assays.

2.2 Development of Fluorescence Assays

The purpose of these assays was to test the hypothesis that the disulfide bond that may exist between C120 and C127 may play a role in fatty acid binding. To begin, two fluorophores were purchased, DAUDA and 1,8-ANS, because of their frequent use in previous publications. DAUDA is implemented less frequently, however its fatty acid tail (Figure 2.3 A) makes it an interesting candidate for the assays. 1,8-ANS is the most commonly used fluorophore to study FABP5, giving a fluorescent signal upon interaction with a hydrophobic environment such as the binding pocket of FABP5.⁸²

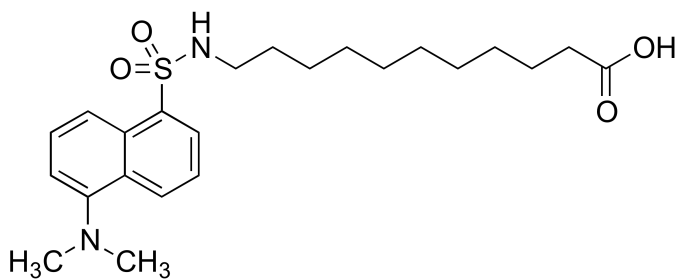
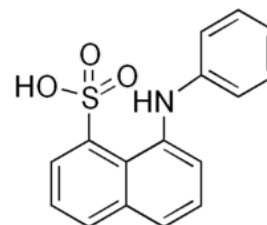
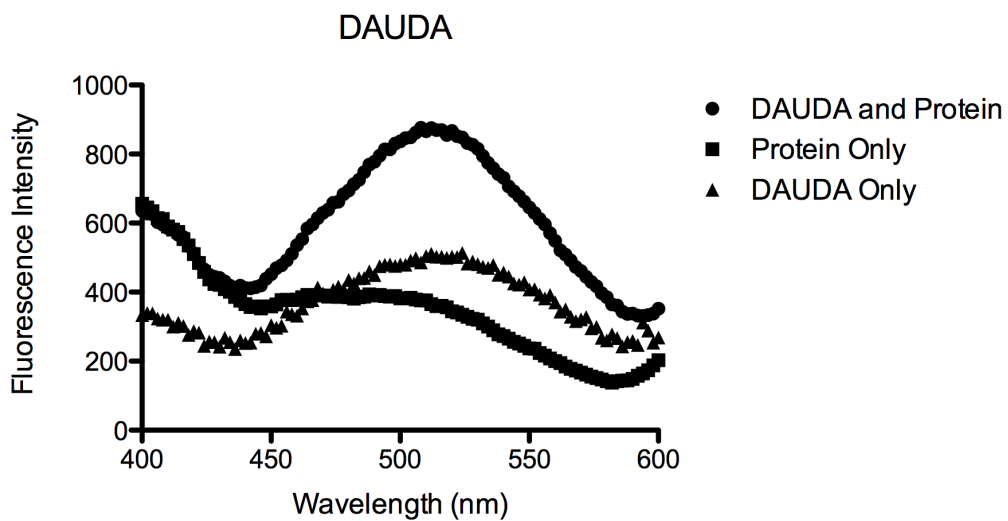
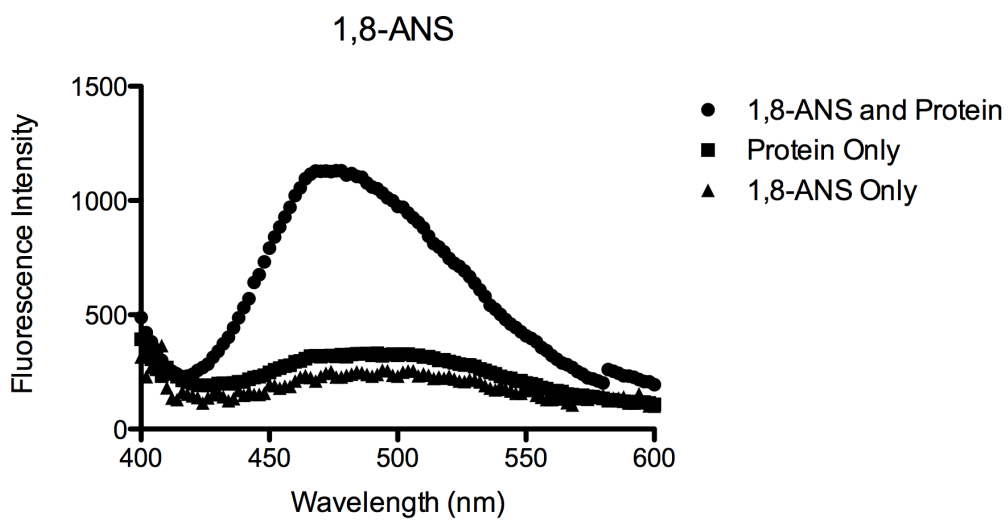
A**B****C****D**

Figure 2.3 Evaluating fluorophores for FABP5 fluorescence assays. The fluorophore structures shown in A and B are DAUDA and 1,8-ANS respectively. The graph, C, depicts the fluorescence of DAUDA with and without protein present (saved as DAUDA development of fluorescence assay). The graph, D, depicts the fluorescence of 1,8-ANS with and without protein present (saved as 1,8-ANS development of fluorescence assays).

After many replicates, the fluorophores 1,8-ANS was chosen for the remaining fluorescence assays. Although DAUDA's fatty acid tail made it a promising candidate to specifically target and fluoresce with FABP5, 1,8-ANS showed a stronger fluorescence signal at the same concentrations and less variability from assay to assay. There is also more published information and established protocols available on the binding of 1,8-ANS to FABP5. The first assay to be performed determined the dissociation constant of 1,8-ANS to WT, C120S, C127S, and C120/127S FABP5 (Figure 2.4). All assays were repeated with three technical and three biological replicates and all analysis was completed using GraphPad Prism 5.0 software.

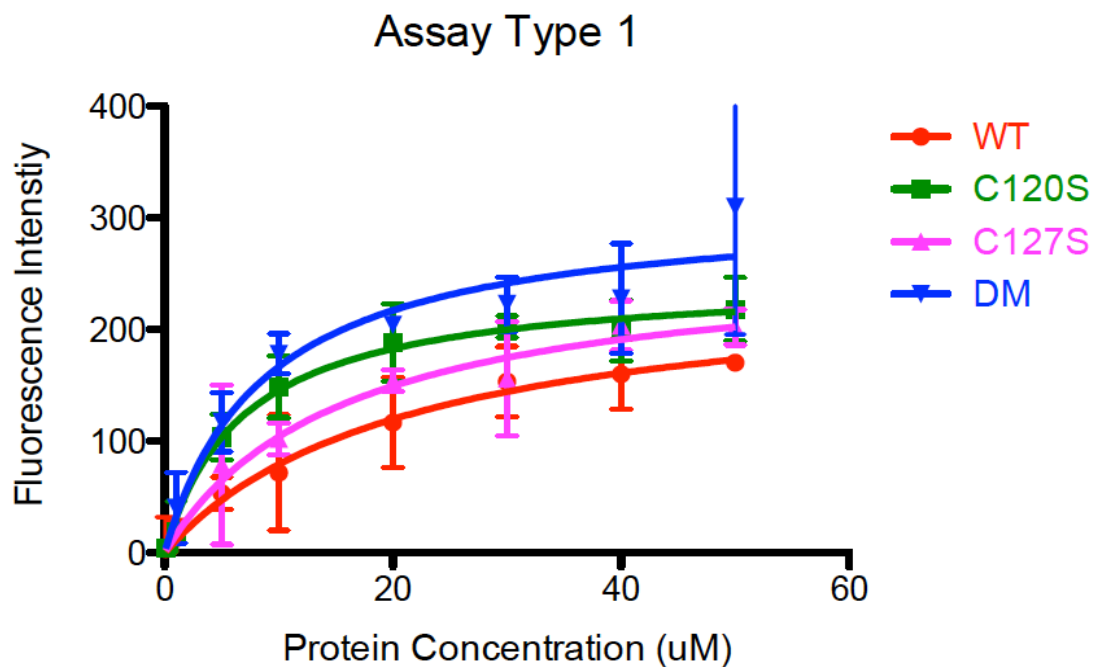
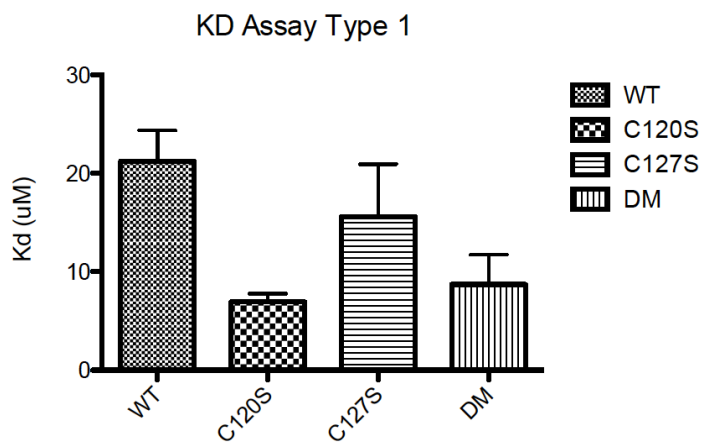
A**B**

Figure 2.4 Assay type 1 with WT and all mutant FABP5. Graph A shows the binding curve of 1,8-ANS to each protein variant as protein concentration increases (saved as Assay Type 1 final graph). Graph B compares the dissociation constant of 1,8-ANS to each protein variant (saved as KD Assay Type 1 final graph).

The dissociation constant of 1,8-ANS with WT, C120S, C127S, and C120/127S is 21.21 μ M \pm 3.148, 6.930 μ M \pm 0.8661, 15.59 μ M \pm 5.349, and 8.709 μ M \pm 3.024 respectively. T-test results indicate that all values are significant except when comparing WT versus C127S protein. Published dissociation constants under the same conditions only exist for WT FABP5 and 1,8-ANS equal to 6.57 μ M.⁷² The discrepancy between the published value and data obtained is something to note, however in this discussion we are more interested in comparing the different protein mutants, specifically C120/127S, to WT FABP5. From these dissociation constants, we can say that the C120S and C120/127S mutants bind the fluorophore the strongest and that the WT protein binds it the weakest.

The second assay performed determined the dissociation constant of 1,8-ANS with WT and C120/127S under different ratios of GSH:GSSG (Figure 2.5). Glutathione is a common tripeptide thiol found in cells that controls oxidation of cysteine residues.⁸³ The concentration of GSH:GSSG was kept at a constant 5mM, the same relative concentration in most mammalian cells.⁸⁴ In these assays, glutathione was chosen due to its physiological relevance with monitoring cysteine oxidation. Three ratios of GSH:GSSG were used (1:10, 1:1, and 10:1) where a ratio of 1:10 denotes 0.5mM GSH to 4.5mM GSSG, 1:1 denotes a ratio of 2.5mM GSH to 2.5mM GSSG, and a ratio of 10:1 is 4.5mM GSH to 0.5mM GSSG. Therefore a 1:10 ratio should oxidize all cysteine residues and a 10:1 ratio should reduce all cysteine residues to free thiols.

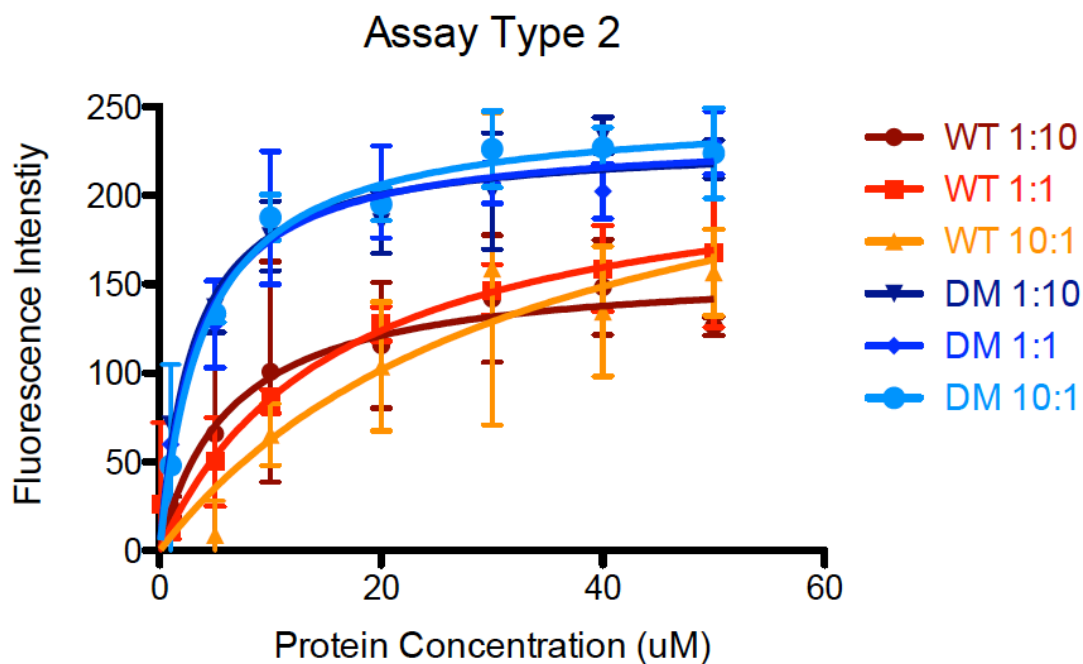
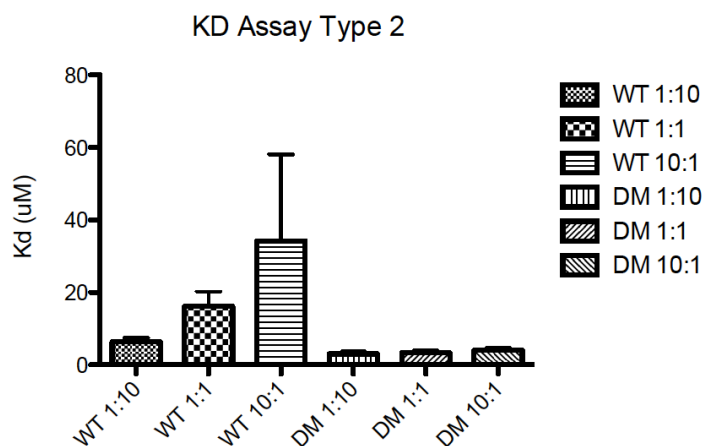
A**B**

Figure 2.5 Assay type 2 with WT and C120/127S FABP5. Graph A shows the binding curve of 1,8-ANS to each protein as protein concentration increases in the presence of different GSH:GSSG ratios (saved as Assay Type 2 final graph). Graph B compares the dissociation constant of 1,8-ANS to each protein under each GSH:GSSG scenario (saved as KD Assay Type 2 final graph).

The dissociation constant of 1,8-ANS with WT FABP5 at 1:10, 1:1, and 10:1 GSH:GSSG is $6.386\mu\text{M} \pm 1.910$, $16.15\mu\text{M} \pm 4.111$, and $34.23\mu\text{M} \pm 23.85$ respectively. The dissociation constant of 1,8-ANS with C120/127S FABP5 is $3.050\mu\text{M} \pm 0.6715$, $3.395\mu\text{M} \pm 0.6682$, and $4.046\mu\text{M} \pm 0.6265$ respectively. T-test results indicate that between all WT samples, the only significant difference is between WT 1:1 and WT 10:1, between all C120/127S samples there is no significance, and between all WT versus C120/127S samples they are all significant. The results of the T-test are interesting because it shows that the difference between WT sample 1:1 and 10:1 are significant however the difference between 1:10 and 10:1 are not. However, the fact that a change in the dissociation constant for the WT protein upon various levels of GSH:GSSG while the C120/127S samples remain constant suggests a potential role for these cysteine residues in protein function.

Finally, the third assay performed determined the binding constant of fatty acid palmitic acid to WT FABP5 and all mutants by out-competing 1,8-ANS (Figure 2.6).

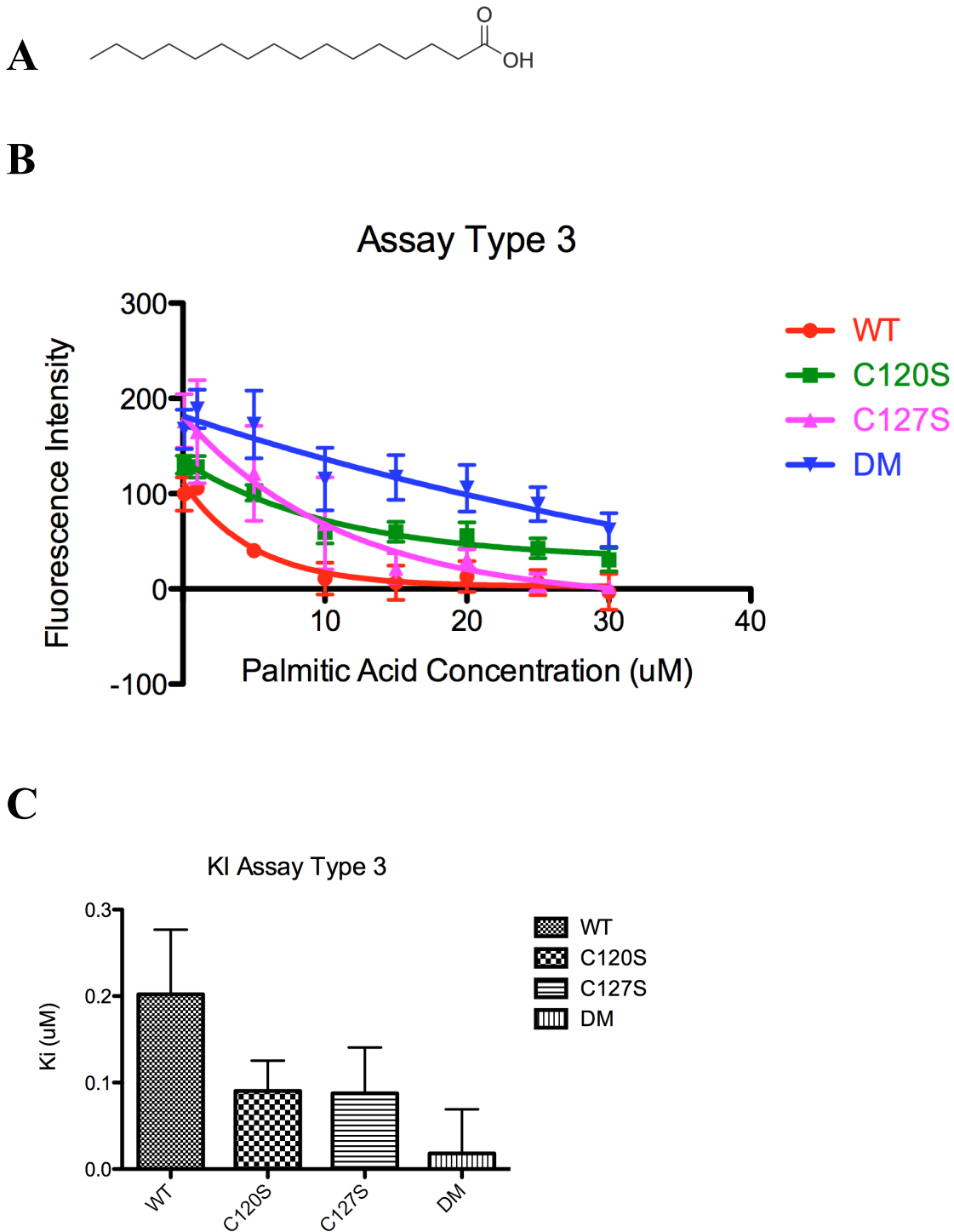


Figure 2.6 Assay type 3 with WT and all mutant FABP5. Picture A shows the structure of palmitic acid used. Graph B shows the competition of 1,8-ANS with palmitic acid as fatty acid concentration is increased for each protein variant (saved as Assay Type

3 final). Graph C compares the binding constant of palmitic acid to each protein variant (saved as KI Assay Type 3 final).

The binding constant of 1,8-ANS with WT, C120S, C127S, and C120/127S FABP5 is $0.2020\mu\text{M} \pm 0.07479$, $0.09048\mu\text{M} \pm 0.03489$, $0.08767\mu\text{M} \pm 0.05300$, and $0.01822\mu\text{M} \pm 0.05098$ respectively. T-test results indicate that all comparisons are significant except for C120S versus C120/127S samples. This assay shows that the mutations made to each cysteine residue affect fatty acid binding to the protein; more specifically that single mutations C120S and C127S have approximately the same effect on reducing binding affinity and that C120/127S has the greatest effect on fatty acid binding. This data suggests that each cysteine residue plays a role in fatty acid binding instead of one specific residue. Therefore a disulfide bond may indeed play a role in stronger fatty acid binding since any implications due to a change in local electronics is nullified as each mutation is to a serine residue. Taking into account the results from Figure 2.5 with Figure 2.6, perhaps the disulfide bond is present and plays a role with both the fluorophore and palmitic acid however the interactions between each of them are different. To test this theory, future experiments should repeat the third assay type under the various GSH:GSSG ratios of assay type 2 to directly observe fatty acid binding in different reductive/oxidative environments. At this point it is important to note that we still cannot definitively state whether a disulfide bond is present and not the effects of a single cysteine residue, but the results thus far have not refuted our hypothesis. Next, we sought to determine the effects of FABP5 expression in cells.

2.3 Expression of FABP5 in Mammalian Cells

The first step in determining the effects of FABP5 expression in mammalian cells is to determine the best cell line to use. Previous work has focused on the use of A431 cells since EGFR is highly overexpressed compared to other cell lines.⁵⁶ However, transfection efficiency with Lipofectamine 2000 is much lower than other cell lines according to ThermoFisher Scientific. Therefore we looked at inherent FABP5 expression within three cell lines as shown in Figure 2.7 to help make the best choice for transfections.

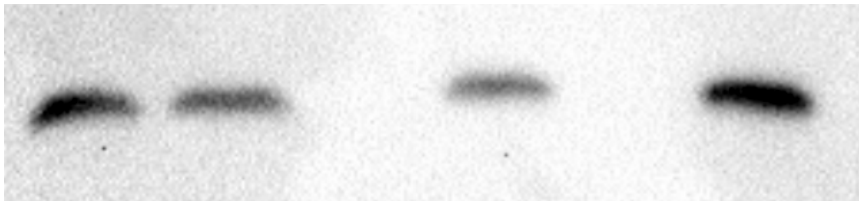


Figure 2.7 Western Blot of FABP5 in various mammalian cell lines. The above figure displays the intrinsic amount of FABP5 produced in three cell lines (from left to right): A431, A431, HEK293T, and SK-OV-3 cells (saved as 11292016).

Therefore since transfection efficiency is the lowest with A431 cells, and the endogenous amount of FABP5 in HEK293T and SK-OV-3 is relatively similar, either cell line would be a viable alternative to use for transfections.

Chapter 3: Conclusions and Future Directions

3.1 Summary of Results and Conclusions

The hypothesis of these experiments was that a disulfide bond might be present between residues C120 and C127 in FABP5 that plays a role in protein function. After completing a multitude of fluorescence assays it is apparent that the WT versus C120/127S FABP5 protein show different trends. Although it appears to support our theory, this data does not completely confirm the presence of a disulfide bond nor can we draw any direct conclusions about how the potential disulfide bond affects protein function. More experiments need to be completed to obtain the full picture of how these residues play a role in FABP5. Future studies should also include experiments within live cells to determine the effects overexpression and knocking out FABP5 has on cellular function as it relates to the EGF signaling pathway.

3.2 Future Directions

3.2.1 Transfections into Mammalian Cells

The next step in exploring the role of FABP5 as it relates to EGF signaling is to transfect mammalian cells to either overexpress the protein (via transient transfections) or knock-down protein expression (via viral transfections). Transient transfections will increase protein expression but the effects will not last. In transient transfections, pcDNA is taken up by cells with the help of a mixture of polycationic and neutral lipids sold as Lipofectamine. The purified pcDNA and Lipofectamine complexes so that the positively charged head group of the lipids interacts with the negatively charged pcDNA.⁸⁵ Once added to cells, the positively charged lipids bring the pcDNA to the

negatively charged cell surface where it can interact with the mammalian cells.⁸⁵ The complex then enters the cell via endocytosis and once in the cell, the pcDNA begins transcription of FABP5.⁸⁵ Other methods to overexpress protein in mammalian cells such as the use of polybrene or electroporation are not as efficient at delivering pcDNA into cells and have poor reproducibility in comparison.⁸⁵ Another transfection method using a lentivirus system creates a stable transfection that lasts, however this is not ideal for protein overexpression. Firstly in viral transfections, pcDNA is integrated into host DNA which is much more difficult to achieve than just translocating foreign pcDNA to the nucleus so there would not be enough pcDNA copies inserted into the host DNA to overexpress the protein. With transient transfections, more copies of pcDNA are translocated to the nucleus thus giving higher amounts of protein expression. Also, the viral packaging vector has a size limit and depending on how large the pcDNA vector is, it might not be a viable option.

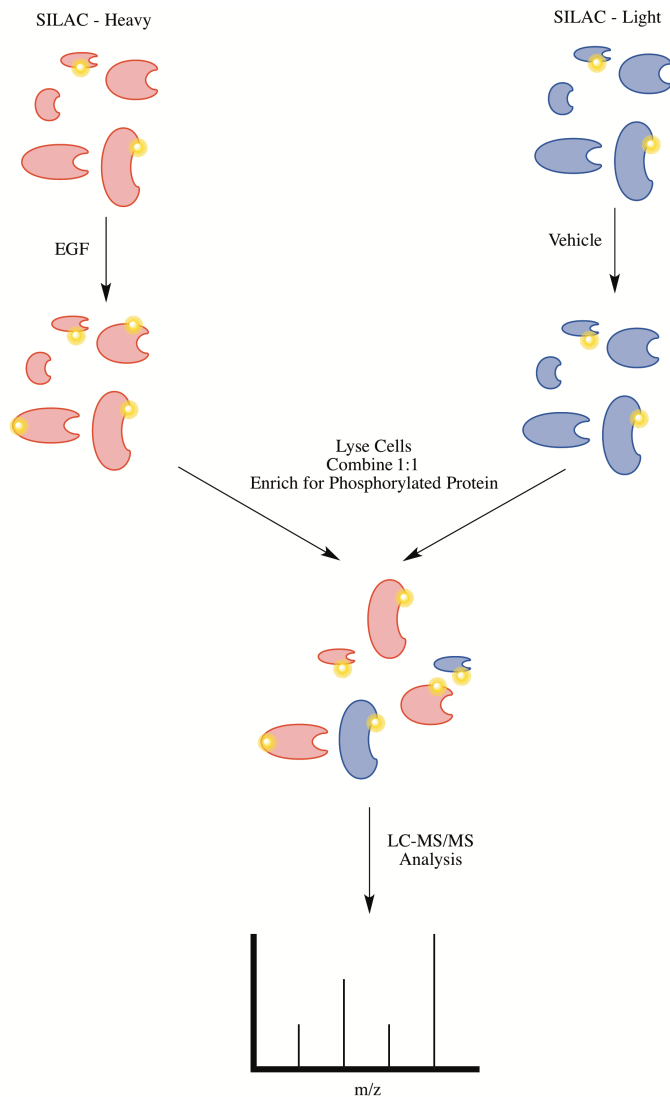
Viral transfections employ a lentiviral system to infect host mammalian cells with DNA that encodes shRNA that is used to knock down the expression of FABP5. In this procedure, a second-generation system is used with three plasmids that separate the necessary components of a functional virus.⁸⁶ Using these plasmids should not produce a continuously replicating virus unless the viral plasmids recombine and the resulting construct is packaged in a virus, which is highly unlikely energetically.⁸⁶ The three plasmids are the transfer vector containing the gene of interest, VSV-G, and psPAX. VSV-G contains the necessary information to produce the envelope protein responsible for determining the specificity of the virus for different cell types via surface glycoproteins and transmembrane proteins.⁸⁶ psPAX contains the necessary information

to produce proteins Gag, Pol, Rev, and Tat which produce the matrix, capsid, and nucleocapsid for Gag, reverse transcriptase and integrase for Pol, helps with nuclear export for Rev, and activates transcription from the LTR promoter for Tat.⁸⁶ Together these plasmids form a viral particle that can insert shRNA for knocking down FABP5 in host cells. The knock down process occurs as shRNA is produced and complexes with the enzyme DICER which removes the hairpin region giving siRNA.⁸⁷ The siRNA is then complexed with RISC, which removes the complementary strand of RNA and targets intracellular mRNA with the complementary strand and degrading it thus knocking out protein expression at the mRNA level.⁸⁷ Other methods of stably knocking down FABP5 expression include the use of other retroviral vectors (which can only infect dividing cells unlike lentivirus which can infect dividing and non-dividing cells) and adeno-associated virus (which requires the use of a helper virus and thus a more complex procedure).⁸⁸ With the overexpression and knock-down of FABP5 protein in mammalian cells, it will be possible to study the role of this protein in EGF activation. An effective way to monitor this would be to observe trends in protein phosphorylation, which is directly affected by EGF stimulation.

3.2.2 Phosphoproteomics

Once human cells have been transfected to either overproduce or knock out FABP5, we can globally analyze the proteome to monitor phosphorylation using mass spectrometry. To do so, phosphorylated proteins have to be tagged, enriched, and prepared for analysis via mass spec. One common method to tag proteins that our lab already has access to is SILAC labeling. This method employs the use of heavy isotopes

incorporated into amino acids used to generate proteins, specifically ^{13}C and ^{15}N into lysine and arginine residues.⁸⁹ So for example, a “heavy” arginine with ^{13}C only would have a 6Da difference from a “light” arginine residue with all ^{12}C . These “heavy” residues are added to culture media fed to cells until all the amino acid residues in proteins have been incorporated as “heavy” residues. A general workflow of how SILAC labeling can be applied to phosphoproteomics is shown in Figure 3.1.



3.1 Workflow for phosphoproteomics studies. The above workflow would be a sufficient method of studying protein phosphorylation on a global scale.

In Figure 3.1, two plates of cells labeled with “heavy” and “light” residues can be used to distinguish phosphorylation events indicated by a yellow circle with and without EGF stimulation. The lysates can then be combined without loss of information and analyzed via mass spec. One of the major challenges though is the enrichment of phosphorylated proteins. Although about a third of the proteome can be phosphorylated at any given time, the level of phosphorylation per protein is varied and specific sites may be phosphorylated anywhere from 1-90%.⁹⁰ Phosphorylated residues include serine, threonine, and tyrosine but using more traditional enrichment methods in phosphoproteomics, tyrosine residues exhibit much fewer hits (less than 1%) via mass spec than physiologically relevant.⁹¹ Traditional methods of phosphorylated protein enrichment center around IMAC and titanium dioxide enrichment. IMAC enrichment is based on the idea that phosphates will be attracted to trivalent metal ions with high affinity. The metal ions are immobilized on a porous column and phosphoproteins are captured and eluted by changing the pH of elution buffer.⁹⁰ The problem with this method is that proteins with many acidic residues, glutamic acid and aspartic acid, also bind to the immobilized metals and co-elute with phosphorylated proteins.⁹⁰ Titanium dioxide enrichment is accomplished by binding phosphoproteins in acidic solution like an anion-affinity exchange column.⁹⁰ The phosphorylated proteins are then eluted using a gradient of alkaline borate buffer containing sodium chloride.⁹⁰ To prevent proteins with many acidic residues without any phosphorylation from binding to the column, 2,5-dihydroxy benzoic acid is added to the protein before being subjected to the column.⁹⁰ In this way, carboxylic acid groups are out-competed while phosphoproteins still bind the

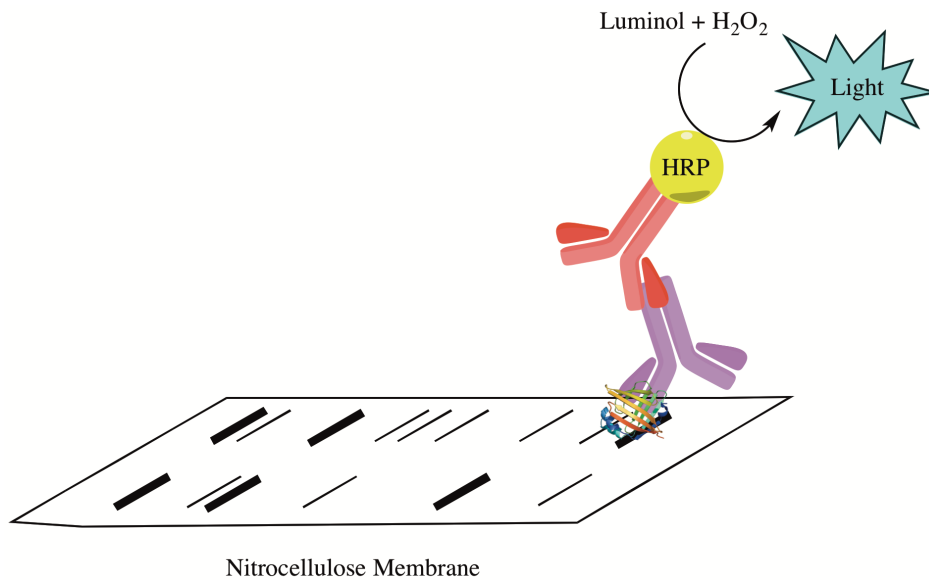
column.⁹⁰ However, neither of these methods address the issue of low tyrosine phosphoprotein counts. Phosphorylated tyrosine residues have a much shorter half-life than serine and threonine residues unless protected by SH2 and PTP domains.⁹¹ Previous methods to enrich phosphorylated tyrosine proteins have focused on antibodies, however due to cost, this was not feasible for large-scale production.⁹² Very recently, a new approach modifying the SH2 domain of Src protein to tightly bind phosphorylated tyrosine residues has been successfully used to increase the amount of phosphotyrosine peptides identified via mass spec.⁹² By making mutations T183V, C188A, and K206L, the SH2 domain binds phosphorylated tyrosine residues with much greater affinity, yielding thousands more hits via mass spec analysis.⁹² This “superbinder” can be mass-produced in *E.coli* and bound to a Ni column to create the final affinity column for phosphotyrosine peptides.⁹² Once the phosphoproteins are collected, the superbinder complexes can be eluted with imidazole, desalted, and separated via acetonitrile with TFA on an IMAC column.⁹² This affinity purification strategy yields accurate and high-throughput data regarding tyrosine phosphorylation in the proteome.

With these enrichment strategies in mind, mass spec analysis for these phosphoproteomics studies will focus on identifying the global changes in protein phosphorylation upon EGF stimulation. Since FABP5 has been shown to oxidize readily due to ROS generated by EGF stimulation, varying the expression levels of FABP5 and the cysteine mutants should yield interesting data regarding proteome phosphorylation since the PPAR β/δ targeted by FABP5 targets the PDK1 gene that phosphorylates AKT and the FABP5 gene.⁷⁵⁻⁷⁶ Such changes within the proteome require high sensitivity and resolution, which cannot be provided by simple LC-MS systems. The use of an LTQ

Orbitrap mass spectrometer is necessary for such delicate studies due to its greatly improved mass accuracy and high resolution over simpler LC-MS models.⁹³ This improvement is a direct result from trapping ions in an electrostatic field via the Orbitrap instead of RF voltage.⁹³ In an LTQ Orbitrap, after ions have been generated, they travel to a linear ion trap where they are stored and ejected as packages thus allowing a continuous source of ions to be used.⁹³ Next they are sent to the C-trap, which is shaped to eliminate any interfering particles and improve the signal-to-noise ratio.⁹³ The C-trap then pulses ions to the Orbitrap with a trajectory that induces an elliptical spin pathway characteristic to each m/z thus giving excellent m/z separation and resolution.⁹³ With such a powerful instrument, LC/LC-MS/MS experiments can be used for these phosphoproteomics studies; however for more specific data regarding singular phosphorylation events on specific components of the EGF pathway, the use of antibodies would be appropriate.

3.2.3 Western Blotting

Another technique that can be used to monitor the role of FABP5 in cells is to observe the phosphorylation of specific components in the EGF signaling pathway. By using western blotting to target specific proteins that are phosphorylated, we can observe changes in phosphorylation at different points in the pathway. Again, ideally A431 cells would be used due to their higher expression levels of EGFR that can be stimulated upon treatment with EGF. The basic premise of western blot imaging via an indirect ELISA technique is shown in Figure 3.2.



3.2 Western Blot technique to monitor protein phosphorylation. Western blotting using antibodies that specifically target phosphorylated proteins can monitor differences in protein phosphorylation for specific proteins in the EGF signaling pathway. The protein shown in this figure is FABP5.

In Figure 3.2, the protein from a cell lysate is immobilized on a nitrocellulose membrane, the protein of interest is targeted with a primary antibody, and a secondary antibody is used to target the primary antibody and provide a measurable signal. Antibodies are inherently highly specific for their antigen so it is possible to have both an antibody for a phosphorylated protein and one without phosphorylation. In this way, qualitative results can be obtained by comparing the amount of phosphorylated to non-phosphorylated protein abundance. To obtain quantitative results, a protein standard must be used in tandem with this experiment. A list of available antibodies available for different components of the EGF signaling pathway is shown in Table 3.1.

Protein of Interest	Site of phosphorylation targeted by antibody on protein	Antibody available
EGFR	None	Anti-EGFR antibody [EP38Y] (ab52894)
EGFR	Y1092	Anti-EGFR (phospho Y1092) antibody [EP774Y] (ab40815)
EGFR	Y1173	Anti-EGFR (phospho Y1173) antibody [E124] (ab32578)
EGFR	Y1086	Anti-EGFR (phospho Y1086) antibody [Y39] (ab32086)
EGFR	Y1068	Anti-EGFR (phospho Y1068) antibody [Y38] (ab32430)
EGFR	Y845	Anti-EGFR (phospho Y845) antibody (ab5636)
EGFR	T693	Anti-EGFR (phospho T693) antibody [EP2256Y] (ab75980)
EGFR	T654	Anti-EGFR (phospho T654) antibody [3F2] (ab78283)
EGFR	S1070 and S1071	Anti-EGFR (phospho S1070 + S1071) antibody [EP2259Y] (ab76300)
EGFR	S1047	Anti-EGFR (phospho S1047) antibody [1H9] (ab24918)
PI3K (p85alpha subunit)	None	Anti-PI 3 Kinase p85 alpha antibody [EPR18702] (ab191606)
PI3K (p85 subunit)	Y607	Anti-PI3K p85 (phospho Y607) antibody (ab182651)
PI3K (p110delta/p85alpha)	None	Recombinant human PI3K (p110 delta/p85 alpha) protein (ab125633)
PI3K (p110delta)	None	Anti-PI 3 Kinase p110 delta antibody (ab1678)

PI3K (p85beta)	Y464	Anti-PI 3 Kinase p85 beta (phospho Y464) antibody (ab138364)
AKT	None	Anti-pan-AKT antibody (ab8805)
AKT	T308	Anti-pan-AKT (phospho T308) antibody (ab38449)
AKT	S473	Anti-AKT1 (phospho S473) antibody (ab66138)
PTEN	None	Anti-PTEN antibody (ab31392)
PTEN	T366	Anti-PTEN (phospho T366) antibody [EP229] (ab109454)
PTEN	S370	Anti-PTEN (phospho S370) antibody (ab30654)
PTEN	S380, T382, T383	Anti-PTEN (phospho S380 + T382 + T383) antibody (ab131107)
PDK1	None but can also detect PDK1 when Y 373 and Y376 are phosphorylated	Anti-PDPK1 antibody [EP569Y] (ab52893)
PDK1	S241	Anti-PDPK1 (phospho S241) antibody (ab32800)
PDK1	S410	Anti-PDPK1 (phospho S410) antibody [EPR6157] (ab133461)
PDK1	Y9	Anti-PDPK1 (phospho Y9) antibody (ab111863)

Table 3.1 List of available antibodies for both phosphorylated and non-phosphorylated components of the EGF signaling pathway. Note this is not a complete list of all antibodies available for the different phosphorylation sites on each protein. All antibodies are produced via Abcam. When performing these experiments, it may be best to choose some, but not all, antibodies to start with in order to gauge how extensively FABP5 affects EGF signaling.

With these assays it would be possible to monitor the amount of phosphorylation of each component in the EGF signaling pathway in cells that have been both virally transfected to knock out the production of FABP5 and cells that have been transiently transfected with FABP5 to overexpress WT, or any FABP5 mutant. It would also be imperative to monitor phosphorylation levels with various amounts of EGF added to cells as well as the length of time cells are subjected to EGF. One major drawback with this proposed series of experiments is the limitation to cell lysates. Protein phosphorylation is very dynamic and more accurate data would be obtained if these experiments were done in living cells.

Procedures for ELISA based assays in living cells have been developed, however due to the amount of disruption at the cell surface and modification to antigens, they may not be a viable option for our studies. For live cell experiments, the cells would have to be fixed and permeabilized to allow the antibodies access inside the cells. Methods for fixation and/or permeabilization of the antigen include organic solvents and cross-linkers.⁹⁴ Organic solvents like methanol and acetone remove lipids and dehydrate the cells causing the proteins to precipitate on the cellular architecture.⁹⁴ Cross-linkers such as paraformaldehyde links together antigens via free amino groups which disrupts cell structure less but alters the antigenicity to where the antibody may not be effective.⁹⁴ This method would then require a permeabilization step, typically accomplished with methanol.⁹⁴ Another change needed for this protocol to work is how signal is obtained. Since we are also interested in studying ROS generation within cells as it relates to EGF signaling, it does not make sense to treat cells with hydrogen peroxide in order to gain signal via luminol interaction with HRP. Therefore a new technique using quantum dots

has been used for excellent signal generation with even the lowest abundance proteins.⁹⁵ The advantages to using quantum dots as a signal are that they are much brighter at lower concentrations, can be specifically excited by one wavelength, are more stable against photobleaching, and can be conjugated to a secondary antibody.⁹⁵ Problems with quantum dot solubility have been overcome via the use of a ZnS-cap and treatment with mercaptoacetic acid.⁹⁵ Other issues that have been solved include bioconjugation to the antibodies. One method of particular interest is the development of a copper free azide-alkyne cycloaddition, “click” chemistry, based strategy where quantum dots that have been capped with an alkyne bearing moiety and the biomolecule is labeled with an azide.⁹⁶

Overall the use of an indirect based ELISA technique with western blotting is useful to determine specific phosphorylation patterns with respect to the components of the EGF signaling pathway. Targeting proteins in living cells would provide more accuracy, however disruption of the cell membrane environment would likely discredit any accuracy gained for specific targets. By using viral and transient transfections to alter FABP5 expression in cells, a multitude of experiments may be performed to determine its effects on protein phosphorylation upon EGF stimulation at both the global and protein-specific scale.

Chapter 4: Materials and Methods

4.1 Cloning and Mutagenesis

	Forward Primer 5'-3'	Reverse Primer 5'-3'	Date Cloning was Successful	Named
WT	GAATTGGATC CAATGGCCAC AGTTCAGC	CTTAAGGTAC CTTACTATTCT ACTTTTTCATA GATCCGAG	17 August, 2015	Ptduet forw fabp5 and ptduet revr fabp5
C120S	CGTCATGAAC AATGTCACCT G	CTCTCCACCAC TAATTTCCCA	22 October, 2015	FABP5_C120 S_fwd and FABP5_C120 S_rev
C127S	CACTCGGATC TATGAAAAG TAGA	CTGGTGACAT TGTTTCATGAC A	22 October, 2015	FABP5_C127 S_fwd and FABP5_C127 S_rev
C120/1 27S	GAAAGATGGG AAATTAGTGG TGGAGAGTGT CATGAACAAT GTCACCAGC	GCTGGTGACA TTGTTTCATGAC ACTCTCCACC ACTAATTTCCC ATCTTTC	9 December, 2015	TY127pres12 0dmfwd and TY127pres12 0dmrev
All into pcDNA	GAATTGGTAC CGCCATGGCC ACAGTTC	CTTAAGGATC CTTACTATTCT ACTTTTTCATA GATCCGAG	30 May, 2016	Fabp5pcdnafo rward and fabp5pcdnare verse

Table 4.1 Primers successfully used for WT and all FABP5 mutants. The name for each primer is what was used when placing the order.

Protocol for Cloning WT FABP5 Into pET-DUET Vector:

1. To dilute primers :

$$500 \times \frac{6000}{\text{primer molecular weight}}$$

= how much water to add (uL) for final primer concentration of 1mg/mL

2. Next dilute primers 1:10 to get a final concentration of 0.1mg/mL

3. Take 1.5uL of 0.1mg/mL primer and add to 50uL total volume PCR reaction
4. Add 1uL of 10ng/uL plasmid template to PCR tube
5. Add 1uL of 10mM dNTPs
6. Add 10uL of pHusion reaction buffer
7. Add 34.5uL sterile water
8. Add 0.5uL pHusion polymerase
9. Cycling conditions for PCR reaction
 1. 5 minutes at 98 °C
 2. 10 seconds at 98 °C
 3. 20 seconds at 61 °C
 4. 45 seconds at 70 °C
 5. repeat steps 2-4 thirty five times
 6. 5 minutes at 70 °C
 7. Leave reaction at 4 °C
10. Perform PCR purification
 1. Add 5 volumes of buffer PB to one volume of PCR reaction and mix
 2. Place a QIAquick column in a 2mL collection tube
 3. To bind DNA, apply the sample to the QIAquick column and centrifuge for 60 seconds, and discard flow-through
 4. To wash, add 750uL of buffer PE, centrifuge for 60 seconds, and discard flow-through
 5. Centrifuge the column one more time for one minute to remove any residual wash buffer

6. Put column in new tube to collect DNA
7. To elute DNA, add 45uL of 1:10 EB buffer in water prewarmed to 42 °C
8. Let stand for five minutes, then centrifuge 1 minute and save flow-through
11. Run an analytical DNA gel using 5uL of PCR reaction and 5uL dye
12. Restriction Digest using the following table to set up each sample (keeping the vector and insert separate):

Volumes	Vector	Insert
Buffer	8uL	6uL
1 st Restriction Enzyme (BamH 1)	4uL	3uL
2 nd Restriction Enzyme (Kpn 1)	4uL	3uL
DNA from PCR	Enough for 2ug	43uL (all purified DNA)
Water	Calculate	5uL
Final Volume	80uL	60uL

Table 4.2 Restriction digest volumes. Remember to keep the vector and insert separate until indicated.

13. Let digestion occur for 1 hour at 37 °C
14. PCR purify and elute vector in 55uL and insert in 30uL of 1:10 EB buffer in water
15. Dephosphorylation of vector only:
 1. Mix 55uL of vector from elution with 4uL cutsmart NEB buffer and 2uL Antarctic phosphatase
 2. Incubate for 30 minutes at 37 °C and PCR purify in the warm room not on the shaker
16. Ligation:

1. Mix 90fM of insert with 30fM vector in 20uL final reaction with 1uL ligase and 2uL buffer diluted to 20uL with water
 2. Incubate for 30 minutes at room temperature
 3. Controls: without insert and without insert but with ligase
 4. Mix entire 20uL of ligation into 50uL competent DH5 α cells and transform
17. Transformation:
1. Incubate 50uL of competent cells on ice for 25 minutes
 2. Heat shock for 45 seconds at 42 °C
 3. Recover on ice for 2 minutes
 4. Add 750uL of LB media
 5. Grow for one hour at 37 °C
 6. Plate 50uL of growth overnight at 37 °C on an LB plate with ampicillin
18. Harvest colonies from sample plates with an inoculation loop and add to 5mL of LB media with ampicillin and allow to grow overnight shaking at 37 °C
19. Miniprep
1. Pellet 5mL overnight bacterial culture by centrifugation (~17,900xg for 1 minute at room temperature)
 2. Resuspend pelleted bacterial cells in 250uL Buffer P1 and transfer to a microcentrifuge tube
 3. Add 250uL Buffer P2 and mix thoroughly by inverting the tube 6 times
 4. Add 350uL Buffer N3 and mix by inverting the tube 6 times
 5. Centrifuge for 10 minutes at 17,900xg at room temperature

6. Apply the supernatant to a QIAprep spin column and centrifuge for 1 minute at 17,900xg
7. Discard flow-through and add 750uL of Buffer PE and centrifuge for another minute at 17,900xg
8. Discard flow-through and centrifuge again for another minute at 17,900xg to remove any remaining buffer
9. Place the QIAprep column in a clean 1.5mL microcentrifuge tube and add 35uL of 1:10 EB buffer in water prewarmed to 42 °C
10. Let stand for 5 minutes at room temperature then spin at 17,900xg for 2 minutes and save the supernatant
20. Take DNA concentrations and prepare samples for sequencing via Genewiz (80ng/uL in 10uL total volume)
21. If sequencing is correct, transform purified DNA into BL21 cells and make glycerol stocks

Protocol for 5' Add-on Mutagenesis for Single Mutations:

1. PCR components:
 1. 1uL of 10ng/uL plasmid
 2. 1.5uL of each primer at 0.1mg/mL
 3. 1uL of 10mM dNTPs
 4. 10uL pHusion buffer
 5. 0.5uL of pHusion polymerase
 6. 34.5uL water

2. Cycling Conditions:
 1. 30 seconds at 98 °C
 2. 10 seconds at 98 °C
 3. 30 seconds at 58 °C for C120S mutant or 30 seconds at 57 °C for C127S mutant
 4. 4 minutes at 72 °C
 5. Repeat steps 2-4 thirty times
 6. 2 minutes at 72 °C
 7. Hold at 4 °C
3. Purify PCR reaction and run DNA analytical gel
4. Phosphorylation:
 1. Reaction Mixture
 1. 2uL PCR prep
 2. 0.5uL T4 polynucleotide kinase
 3. 2.5uL of 10x ligase buffer (not kinase buffer since it doesn't have ATP)
 4. 20.5uL water
 2. Incubations
 1. 30 minutes at 37 °C
 2. 10 minutes at 70 °C to deactivate the kinase
 3. Hold at 4 °C
5. Ligation
 1. Reaction Mixture
 1. 3.5uL phosphorylation reaction

2. 0.5uL T4 ligase
3. 4uL of 5x ligation buffer
4. 12uL water
2. Incubate at room temperature for 30 minutes
6. Transform into DH5 α cells
7. Inoculate colonies and sequence results
8. Transform DNA into BL21 cells

Protocol for Lightning Mutagenesis for C120/127S Mutant:

1. PCR reaction components:
 1. 2.5uL of 10x reaction buffer
 2. xuL (50ng) of DNA template
 3. xuL (62.5ng) of primer #1
 4. xuL (62.4ng) of primer #2
 5. 0.5uL of dNTP mix
 6. 0.75uL of QuikSolution reagent
 7. Add 1uL DMSO
 8. Add enough water for a final volume of 25uL
 9. Add 0.5uL QuikChange Lightning Enzyme
2. Cycling Conditions:
 1. 2 minutes at 95 °C
 2. 20 seconds at 95 °C
 3. 1 minute at 60 °C

4. 6 minutes at 68 °C
 5. Repeat steps 2-4 eighteen times
 6. 5 minutes at 68 °C
 7. Hold at 4 °C
3. Dpn1 Digest:
1. Add 2uL of Dpn1 restriction enzyme directly to each PCR reaction
 2. Mix by pipetting up and down
 3. Incubate at 37 °C for 5 minutes
 4. Transformation:
 1. Thaw the XL10-Gold competent cells on ice
 2. Aliquot 22.5uL cells per PCR into a pre-chilled tube
 3. Add 1uL of the β -ME mix provided
 4. Swirl and incubate on ice for 2 minutes
 5. Add 1uL of Dpn1 digested PCR to cells
 6. Incubate on ice for 30 minutes
 7. Preheat NZY⁺ broth in a 42 °C water bath
 8. Heat pulse tubes in 42 °C for 30 seconds
 9. Incubate on ice for 2 minutes
 10. Add 0.25mL preheated NZY⁺ broth to each tube
 11. Incubate at 37 °C for 1 hour shaking
 12. Plate 200uL of reaction mixture on to plates
 5. Inoculate colonies, miniprep and sequence results
 6. Transform purified DNA into BL21 cells

Protocol for Putting FABP5 into pcDNA:

1. Designed primers with different restriction enzyme cut sites than FABP5 in pET-DUET vector. For the forward primer used HindIII restriction enzyme and for the reverse primer used XbaI restriction enzyme. Also included Kozak sequence on the forward primer (CCGCC) to promote better expression in mammalian cells
2. Used the same PCR reagents as listed for cloning WT FABP5 into pET-DUET except that the plasmid was purified FABP5 (WT and all mutants) in pET-DUET. Primers used were also diluted the same way
3. Cycling Conditions:
 1. 5 minutes at 98 °C
 2. 10 seconds at 98 °C
 3. 30 seconds at 60 °C
 4. 1 minute at 70 °C
 5. Repeat steps 2-4 thirty four times
 6. 5 minutes at 70 °C
 7. Hold at 4 °C
4. The rest of the procedure is identical to the procedure for putting WT FABP5 into pET-DUET. The only changes are the restriction enzymes used during the restriction digest and the vector used is purified pcDNA 3.1(+).A.

4.2 Bacterial and Mammalian Cell Culture

Protocol for Large Scale Growths of All FABP5:

1. Prepare 5mL overnight samples from glycerol stocks
 1. Add 5mL LB media containing 100uM ampicillin to a 15mL conical tube
 2. Dip an inoculation loop into glycerol stock and then place in sample tube
 3. Let grow overnight shaking at 37 °C
2. Autoclave 500mL of LB media in a 2L Erlenmeyer flask for each protein sample and let cool overnight
3. Add ampicillin to 2L flasks containing media until final concentration equals 100uM
4. Add 5mL overnight samples to each 2L flask of LB media and grow to an OD600 of ~0.7-1.0
5. Add IPTG to a final concentration of 1mM and let the 2L flasks swirl at 37 °C overnight
6. Spin down bacterial growths using 50mL conical tubes for 15 minutes at 5000rpm
7. Add 9mL of PBS to each cell pellet and pipette to completely resuspend before lysing
8. Lyse bacteria at 95% amplitude 3x 20 buzzes each
9. Aliquot bacteria lysates to 2mL microcentrifuge tubes and balance (should be able to fit one pellet into a total of four tubes)
10. Centrifuge lysates in the cold room for 30 minutes at 1400xg
11. Save the supernatant
12. Purification via nickel columns:

1. Prepare nickel columns by adding 2mL of Ni resin to each column and allowing gravity to remove buffer
 2. Wash three times with water via gravity flow
 3. Wash three times with PBS via gravity flow
 4. Add saved supernatant to the column (only one type of protein per column to minimize any chance of contamination) and allow protein to bind the column via gravity flow. Do not force protein through the column; this will take a substantial amount of time. If the column appears clogged, gently resuspend the top layer of nickel resin until the flow returns but only if the column will not flow
 5. Add 3mL of 25mM imidazole to each column and elute all protein without a His-tag via gravity flow
 6. Add 2.5mL of 250mM imidazole to each column and collect the eluent
 7. Wash each column three times with PBS via gravity flow then store capped in the 4 °C fridge
13. Purification via PD10 columns:
1. Remove the cap and cut the tip off of each PD10 column. Use one column per protein sample and do not reuse them
 2. Allow the column buffer to flow through via gravity
 3. Wash the column three times with PBS at pH 8.2 via gravity
 4. Apply saved Ni column eluent and discard flow-through
 5. Add 3mL of PBS (pH 8.2) and save the eluent
 6. Discard PD10 columns

14. Purification via Hydroxyalkoxypropyl Dextran columns:

1. Add hydroxyalkoxypropyl dextran powder to the 2mL mark of each column
2. Fill the column with acetone to pack the powder and allow it to flow through via gravity
3. Wash column with PBS (pH 8.2) via gravity
4. Apply sample from PD10 column to hydroxyalkoxypropyl dextran column and collect the fully purified supernatant

15. Determine protein concentration via Bradford assay

16. Store all protein samples in the cold room

Protocol for Mammalian Cell Culture:

1. The three cell types previously described are all cultured differently:

1. A431 cells require complete DMEM (addition of FBS and PSA) and the media has to be replaced on a specific schedule (on the third day since the last passage, the fifth day, the sixth day, then every day until they are confluent enough to be passaged). If the cells are not monitored closely, the plate will suddenly die and a new stock must be thawed. These cells also appear to have difficulty surviving past approximately 20-30 passages. These cells are very difficult to remove from the plate with trypsin and may take over 30 minutes to begin to lift off of the plate
2. SK-OV-3 cells require complete RPMI (addition of FBS and PSA) and the media to be replaced 1-2 times between passages. These cells are easy to passage, requiring only ten minutes in trypsin to be removed from the plate.

They are also fully confluent in about a week's time depending on how many cells were initially plated (about 20% of a 10cm diameter plate should be confluent in one week)

3. HEK293T cells require complete DMEM (addition of FBS and PSA) and the media to be replaced maybe once before the next passage since they grow rapidly. These cells are easy to passage, requiring only ten minutes in trypsin to be removed from the plate. They are also fully confluent within days depending on how many cells were initially plated (about 20% of a 10cm diameter plate should be confluent in 2-3 days)
2. To remove cells from the plate surface, trypsin is used
 1. Remove all media from the plate
 2. Add 4mL trypsin to a 10cm diameter plate of cells so that they are all covered
 3. Allow plates of cells to incubate at 37 °C for ten minutes
 4. If the cells aren't lifting off the plate, add another 1mL of trypsin and incubate for another 5 minutes
 5. Once all cells are floating in trypsin, add 10mL of the appropriate media to the plate and collect all of the cells in 15mL conical tubes
 6. Spin cells down for 4 minutes at 200xg
 7. Remove all media and add fresh media to cell pellet
 8. Resuspend cell pellet and aliquot into new plates with fresh media
 9. Store all mammalian cells in 37 °C incubator

4.3 Analytical Methods

Protocol for Assay Type 1:

1. Dilute 1,8-ANS stock (250uM) to 50uM in ethanol
2. Calculate protein dilutions for each concentration in 100uL total volume (0.1, 1, 5, 10, 20, 30, 40, 50uM protein)
3. Calculate the amount of PBS (pH 8.2) to add to protein to reach a total volume of 99uL
4. Add PBS (pH 8.2) first then add protein, pipetting up and down every time to thoroughly mix. Also do not add samples to wells around the outside of the plate reader plate (only rows B-G and columns 2-11 are used)
5. Add 1uL of 50uM 1,8-ANS for a final concentration of 500nM 1,8-ANS and only 1% ethanol in the final sample. Remember to pipette up and down to mix thoroughly and use a fresh pipette every time to avoid contamination
6. Make blank samples with only protein in PBS (add 1uL pure ethanol instead of 1,8-ANS to keep the amount of ethanol constant)
7. Make each sample three times for three technical replicates per plate
8. Repeat with two more growths for three biological replicates
9. Settings on plate reader:
 1. Endpoint, Fluorescence, bottom read
 2. Excitation wavelength = 380nm
 3. Emission wavelength = 460nm
 4. Temperature set to 37 °C
 5. No Auto Cutoff

6. Sensitivity set to automatic and 5 readings
7. Automix before the first read for 60 seconds
8. Select the plate type as 96 Well Greiner blk/clrbtm
9. Select reading area on the plate and hit ok

Protocol for Assay Type 2:

1. Dilute 1,8-ANS stock (250uM) to 50uM in ethanol
2. Make stocks of GSH:GSSG
 1. 1:10 ratio as 25mM GSH with 225mM GSSG in water
 2. 1:1 ratio as 125mM GSH with 125mM GSSG in water
 3. 10:1 ratio as 225mM GSH with 25mM GSSG in water
 4. For each sample at a specific GSH:GSSG ratio, to get the appropriate concentration in each well add 2uL of the corresponding stock
3. Calculate protein dilutions for each concentration in 100uL total volume (0.1, 1, 5, 10, 20, 30, 40, and 50uM protein) only using WT and C120/127S protein
4. Calculate the amount of PBS (pH 8.2) to add to protein to reach a total volume of 97uL
5. Add PBS (pH 8.2) first then add protein to each well, pipetting up and down every time to thoroughly mix
6. Add 2uL GSH:GSSG stock to each well, pipetting thoroughly and using a fresh pipette tip each time
7. Duplicate these sample wells for the blank samples and make each in triplicate for three technical replicates

8. Incubate plate in the warm room at 37 °C for one hour
9. Add 1uL of 50uM 1,8-ANS to sample wells
10. For blank samples do not include fluorophore; instead add 1uL ethanol to keep ethanol concentration constant at 1% and final volume at 100uL
11. Read using same plate reader settings as the protocol for Assay Type 1

Protocol for Assay Type 3:

1. Dilute 1,8-ANS stock (250uM) to 100uM in ethanol
2. Dilute stocks of different palmitic acid concentrations in ethanol that will have the following concentrations when 0.5uL is added to 100uL total volume: 0.1, 1, 5, 10, 15, 20, 25, and 30uM palmitic acid
3. Calculate protein dilutions for 10uM in 100uL total volume
4. Calculate the amount of PBS (pH 8.2) to add to protein to reach a total volume of 99uL
5. Add PBS (pH 8.2) first then add protein to each well, pipetting up and down every time to thoroughly mix
6. For blank samples, only add 99uL PBS
7. Add 0.5uL palmitic acid stock to each well, pipetting thoroughly and using a fresh pipette tip each time
8. Immediately add 0.5uL of 100uM 1,8-ANS to sample wells and to wells used for blanks with just palmitic acid
9. Read using same plate reader settings as the protocol for Assay Type 1

Protocol for Western Blot:

1. Run protein on an SDS-PAGE gel (15%)
 1. Gel Recipe for 15% (Top Layer enough for 4 gels):
 - 14.9mL water
 - 3.33mL Acrylamide
 - 6.25mL of 0.5M Tris (pH 6.8)
 - 250uL of 10% SDS in water
 - 250uL of 10% APS in water
 - 25uL TEMED
 2. Gel Recipe for 15% (Bottom Layer enough for 4 gels):
 - 9.2mL water
 - 20mL Acrylamide
 - 10mL of 1.5M Tris (pH 8.8)
 - 400uL of 10% SDS in water
 - 400uL of 10% APS in water
 - 40uL TEMED
 3. Combine all components for top and bottom layers except for APS
 4. Set up gel apparatus and fill with bottom layer (with APS added) almost to the top
 5. Fill the rest of the gel with ethanol and wait about 45 minutes
 6. Add APS to the top layer and pipette top layer to gel
 7. Add comb to define the wells and let sit for 45 minutes
 8. Remove comb and wrap gels in wet paper towels and store in the 4 °C fridge

9. To use, place gel in gel box and fill with running buffer
 10. Determine protein concentration desired in 50uL and make samples diluted with PBS
 11. Add 50uL of 2x loading dye to each sample and mix thoroughly
 12. Create ladder sample to determine protein size when gel is finished by adding 20uL of 2x loading dye to "R" ladder
 13. Aliquot all 25uL of "R" ladder into one well on the side of the gel
 14. Aliquot 50uL of protein samples into each well of the gel
 15. Place the lid on the gel box and run for 170 minutes at 100 volts and 400 amps
2. Transfer protein to membrane:
1. Fill the tub provided with transfer buffer from the cold room
 2. Create a sandwich using the western cassette
 1. Order of the sandwich: black side of the cassette -> black sponge -> filter paper -> gel with protein on it -> nitrocellulose membrane (do not touch with fingers) -> filter paper -> black sponge -> clear side of cassette
 2. Use a glass pipette to smooth out the gel->membrane interface so it is free of any bubbles
 3. Close the cassette and put the black side facing the black part of the holder that connects it to the voltage in the gel box and put the clear side of the cassette next to the red side of the holder
 4. Place an ice pack in the box
 5. Fill the gel box with transfer buffer

6. Run gel for 120 minutes at 70 volts
3. When done, remove the membrane and wash for 5 minutes with TBST shaking
4. Add ponceau stain to visualize protein lanes and to make sure the protein transferred
5. Remove dye by washing membrane three times for 5 minutes each with TBST buffer while shaking
6. Next add 2.5g of powdered milk in 50mL TBST to the membrane and let it shake for two hours at room temperature
7. Once done, wash the membrane again three times for 5 minutes each with TBST buffer while shaking
8. Allow the membrane to be exposed to the primary antibody (FABP5 rabbit antibody diluted 1:1000 in TBST) overnight at 4 °C in the cold room while shaking
9. The next day, wash the membrane again three times for 5 minutes each with TBST buffer while shaking
10. Add secondary (anti-rabbit) antibody and allow it to shake at room temperature for 2 hours
11. Wash the membrane again three times for 5 minutes each with TBST buffer while shaking
12. Image with high sensitivity on the Bio-RAD ChemiDoc MP Imaging System
13. Note that all antibodies can be used multiple times (about 3-4 uses) so save them after each use

References:

1. Wang, Dingzhi, Dianren Xia, and Raymond N. DuBois. "The crosstalk of PTGS2 and EGF signaling pathways in colorectal cancer." *Cancers* 3.4 (2011): 3894-3908.
2. Savage, C. Richard, John H. Hash, and Stanley Cohen. "Epidermal growth factor location of disulfide bonds." *Journal of Biological Chemistry* 248.22 (1973): 7669-7672.
3. Goodsell, David S. "The molecular perspective: epidermal growth factor." *The oncologist* 8.5 (2003): 496-497.
4. Scaltriti, Maurizio, and José Baselga. "The epidermal growth factor receptor pathway: a model for targeted therapy." *Clinical Cancer Research* 12.18 (2006): 5268-5272.
5. Joh, Eun-Ha, et al. "Pleckstrin homology domain of Akt kinase: A proof of principle for highly specific and effective non-enzymatic anti-cancer target." *PLoS one* 7.11 (2012): e50424.
6. Hemmings, Brian A., and David F. Restuccia. "Pi3k-pkb/akt pathway." *Cold Spring Harbor perspectives in biology* 4.9 (2012): a011189.
7. Stambolic, Vuk, et al. "Negative regulation of PKB/Akt-dependent cell survival by the tumor suppressor PTEN." *Cell* 95.1 (1998): 29-39.
8. Huang, Jingxiang, and Brendan D. Manning. "The TSC1–TSC2 complex: a molecular switchboard controlling cell growth." *Biochemical Journal* 412.2 (2008): 179-190.
9. Tafani, Marco, et al. "Induction of the mitochondrial permeability transition mediates the killing of HeLa cells by staurosporine." *Cancer research* 61.6 (2001): 2459-2466.
10. Tzivion, Guri, Melissa Dobson, and Gopalakrishnan Ramakrishnan. "FoxO transcription factors; Regulation by AKT and 14-3-3 proteins." *Biochimica et Biophysica Acta (BBA)-Molecular Cell Research* 1813.11 (2011): 1938-1945.
11. Threadgill, David W., et al. "Targeted disruption of mouse EGF receptor: effect of genetic background on mutant phenotype." *Science* 269.5221 (1995): 230.
12. Jorissen, Robert N., et al. "Epidermal growth factor receptor: mechanisms of activation and signalling." *Experimental cell research* 284.1 (2003): 31-53.
13. Sugawa, Noriaki, et al. "Identical splicing of aberrant epidermal growth factor receptor transcripts from amplified rearranged genes in human glioblastomas." *Proceedings of the National Academy of Sciences* 87.21 (1990): 8602-8606.
14. Ekstrand, A. Jonas, et al. "Amplified and rearranged epidermal growth factor receptor genes in human glioblastomas reveal deletions of sequences encoding portions of the N-and/or C-terminal tails." *Proceedings of the National Academy of Sciences* 89.10 (1992): 4309-4313.
15. Schlegel, Jurgen, et al. "Amplification of the epidermal - growth - factor - receptor gene correlates with different growth behaviour in human glioblastoma." *International journal of cancer* 56.1 (1994): 72-77.
16. Moscatello, David K., et al. "Frequent expression of a mutant epidermal growth factor receptor in multiple human tumors." *Cancer research* 55.23 (1995): 5536-5539.
17. Vassar, Robert, and Elaine Fuchs. "Transgenic mice provide new insights into the role of TGF- α during epidermal development and differentiation." *Genes & Development* 5.5 (1991): 714-727.
18. Dominey, Andrea M., et al. "Targeted overexpression of transforming growth factor alpha in the epidermis of transgenic mice elicits hyperplasia, hyperkeratosis, and spontaneous, squamous papillomas." *Cell growth & differentiation: the molecular biology journal of the American Association for Cancer Research* 4.12 (1993): 1071-1082.
19. Lynch, Thomas J., et al. "Activating mutations in the epidermal growth factor receptor underlying responsiveness of non-small-cell lung cancer to gefitinib." *New England Journal of Medicine* 350.21 (2004): 2129-2139.
20. Pao, William, et al. "Acquired resistance of lung adenocarcinomas to gefitinib or erlotinib is associated with a second mutation in the EGFR kinase domain." *PLoS Med* 2.3 (2005): e73.
21. Hubbard, Stevan R. "EGF receptor inhibition: attacks on multiple fronts." *Cancer cell* 7.4 (2005): 287-288.
22. Brown, Jennifer R., et al. "Idelalisib, an inhibitor of phosphatidylinositol 3-kinase p110 δ , for relapsed/refractory chronic lymphocytic leukemia." *Blood* 123.22 (2014): 3390-3397.
23. Walker, Edward H., et al. "Structural determinants of phosphoinositide 3-kinase inhibition by wortmannin, LY294002, quercetin, myricetin, and staurosporine." *Molecular cell* 6.4 (2000): 909-919.

24. Morris, Luc GT, and Timothy A. Chan. "Therapeutic targeting of tumor suppressor genes." *Cancer* 121.9 (2015): 1357-1368.
25. Nagata, Yoichi, et al. "PTEN activation contributes to tumor inhibition by trastuzumab, and loss of PTEN predicts trastuzumab resistance in patients." *Cancer cell* 6.2 (2004): 117-127.
26. Hirai, Hiroshi, et al. "MK-2206, an allosteric Akt inhibitor, enhances antitumor efficacy by standard chemotherapeutic agents or molecular targeted drugs in vitro and in vivo." *Molecular cancer therapeutics* 9.7 (2010): 1956-1967.
27. Arceci, Robert J., et al. "A phase IIa study of afuresertib, an oral pan - AKT inhibitor, in patients with Langerhans cell histiocytosis." *Pediatric Blood & Cancer* (2016).
28. Romorini, Leonardo, et al. "AKT/GSK3 β signaling pathway is critically involved in human pluripotent stem cell survival." *Scientific Reports* 6 (2016).
29. Feldman, Morris E., et al. "Active-site inhibitors of mTOR target rapamycin-resistant outputs of mTORC1 and mTORC2." *PLoS Biol* 7.2 (2009): e1000038.
30. Hudes, Gary, et al. "Temsirrolimus, interferon alfa, or both for advanced renal-cell carcinoma." *New England Journal of Medicine* 356.22 (2007): 2271-2281.
31. Motzer, Robert J., et al. "Efficacy of everolimus in advanced renal cell carcinoma: a double-blind, randomised, placebo-controlled phase III trial." *The Lancet* 372.9637 (2008): 449-456.
32. Bae, Yun Soo, et al. "Epidermal growth factor (EGF)-induced generation of hydrogen peroxide Role in EGF receptor-mediated tyrosine phosphorylation." *Journal of Biological Chemistry* 272.1 (1997): 217-221.
33. Truong, Thu H., and Kate S. Carroll. "Redox regulation of epidermal growth factor receptor signaling through cysteine oxidation." *Biochemistry* 51.50 (2012): 9954-9965.
34. Stone, James R., and Suping Yang. "Hydrogen peroxide: a signaling messenger." *Antioxidants & redox signaling* 8.3-4 (2006): 243-270.
35. Kwon, Jaeyul, et al. "Reversible oxidation and inactivation of the tumor suppressor PTEN in cells stimulated with peptide growth factors." *Proceedings of the National Academy of Sciences of the United States of America* 101.47 (2004): 16419-16424.
36. Bienert, Gerd P., Jan K. Schjoerring, and Thomas P. Jahn. "Membrane transport of hydrogen peroxide." *Biochimica et Biophysica Acta (BBA)-Biomembranes* 1758.8 (2006): 994-1003.
37. Bienert, Gerd P., et al. "Specific aquaporins facilitate the diffusion of hydrogen peroxide across membranes." *Journal of Biological Chemistry* 282.2 (2007): 1183-1192.
38. Miller, Evan W., Bryan C. Dickinson, and Christopher J. Chang. "Aquaporin-3 mediates hydrogen peroxide uptake to regulate downstream intracellular signaling." *Proceedings of the National Academy of Sciences* 107.36 (2010): 15681-15686.
39. Lambeth, J. David. "NOX enzymes and the biology of reactive oxygen." *Nature Reviews Immunology* 4.3 (2004): 181-189.
40. Lee, Seung-Rock, et al. "Reversible inactivation of the tumor suppressor PTEN by H₂O₂." *Journal of Biological Chemistry* 277.23 (2002): 20336-20342.
41. Denu, John M., and Jack E. Dixon. "Protein tyrosine phosphatases: mechanisms of catalysis and regulation." *Current opinion in chemical biology* 2.5 (1998): 633-641.
42. Halvey, Patrick J., et al. "Compartmental oxidation of thiol-disulphide redox couples during epidermal growth factor signalling." *Biochemical Journal* 386.2 (2005): 215-219.
43. Peskin, Alexander V., et al. "The high reactivity of peroxiredoxin 2 with H₂O₂ is not reflected in its reaction with other oxidants and thiol reagents." *Journal of Biological Chemistry* 282.16 (2007): 11885-11892.
44. Winterbourn, Christine C. "Reconciling the chemistry and biology of reactive oxygen species." *Nature chemical biology* 4.5 (2008): 278-286.
45. Weerapana, Eranthie, et al. "Quantitative reactivity profiling predicts functional cysteines in proteomes." *Nature* 468.7325 (2010): 790-795.
46. Beinert, Helmut, Richard H. Holm, and Eckard Münck. "Iron-sulfur clusters: nature's modular, multipurpose structures." *Science* 277.5326 (1997): 653-659.
47. Boatright, Kelly M., and Guy S. Salvesen. "Mechanisms of caspase activation." *Current opinion in cell biology* 15.6 (2003): 725-731.
48. Paulsen, Candice E., et al. "Peroxide-dependent sulfenylation of the EGFR catalytic site enhances kinase activity." *Nature chemical biology* 8.1 (2012): 57-64.
49. Wang, He, et al. "In Vitro Assembly and Structure of Trichocyte Keratin Intermediate Filaments A Novel Role for Stabilization by Disulfide Bonding." *The Journal of cell biology* 151.7 (2000): 1459-1468.

50. Rhee, Sue Goo, et al. "Intracellular messenger function of hydrogen peroxide and its regulation by peroxiredoxins." *Current opinion in cell biology* 17.2 (2005): 183-189.
51. Zhang, Jianming, Priscilla L. Yang, and Nathanael S. Gray. "Targeting cancer with small molecule kinase inhibitors." *Nature Reviews Cancer* 9.1 (2009): 28-39.
52. Wani, Revati, et al. "Isoform-specific regulation of Akt by PDGF-induced reactive oxygen species." *Proceedings of the National Academy of Sciences* 108.26 (2011): 10550-10555.
53. Murata, Hiroaki, et al. "Glutaredoxin exerts an antiapoptotic effect by regulating the redox state of Akt." *Journal of Biological Chemistry* 278.50 (2003): 50226-50233.
54. Couvertier, Shalise M., Yani Zhou, and Eranthie Weerapana. "Chemical-proteomic strategies to investigate cysteine posttranslational modifications." *Biochimica et Biophysica Acta (BBA)-Proteins and Proteomics* 1844.12 (2014): 2315-2330.
55. Weerapana, Eranthie, Anna E. Speers, and Benjamin F. Cravatt. "Tandem orthogonal proteolysis-activity-based protein profiling (TOP-ABPP)—a general method for mapping sites of probe modification in proteomes." *Nature protocols* 2.6 (2007): 1414-1425.
56. Abo, Masahiro, and Eranthie Weerapana. "A Caged Electrophilic Probe for Global Analysis of Cysteine Reactivity in Living Cells." *Journal of the American Chemical Society* 137.22 (2015): 7087-7090.
57. Smathers, Rebecca L., and Dennis R. Petersen. "The human fatty acid-binding protein family: evolutionary divergences and functions." *Human genomics* 5.3 (2011): 1.
58. Furuhashi, Masato, and Gökhan S. Hotamisligil. "Fatty acid-binding proteins: role in metabolic diseases and potential as drug targets." *Nature reviews Drug discovery* 7.6 (2008): 489-503.
59. Veerkamp, Jacques H., and Ronald GHJ Maatman. "Cytoplasmic fatty acid-binding proteins: their structure and genes." *Progress in lipid research* 34.1 (1995): 17-52.
60. Hohoff, Carsten, et al. "Expression, purification, and crystal structure determination of recombinant human epidermal-type fatty acid binding protein." *Biochemistry* 38.38 (1999): 12229-12239.
61. Gutiérrez-González, Luis H., et al. "Solution structure and backbone dynamics of human epidermal-type fatty acid-binding protein (E-FABP)." *Biochemical Journal* 364.3 (2002): 725-737.
62. Yamazaki, Shingo, et al. "Incorporation of plasma [¹⁴C] palmitate into the hypoglossal nucleus following unilateral axotomy of the hypoglossal nerve in adult rat, with and without regeneration." *Brain research* 477.1-2 (1989): 19-28.
63. Marcelino, Anna Marie C., Robert G. Smock, and Lila M. Gierasch. "Evolutionary coupling of structural and functional sequence information in the intracellular lipid-binding protein family." *Proteins: Structure, Function, and Bioinformatics* 63.2 (2006): 373-384.
64. Ek, Bengt A., et al. "Fatty acid binding proteins reduce 15-lipoxygenase-induced oxygenation of linoleic acid and arachidonic acid." *Biochimica et Biophysica Acta (BBA)-Lipids and Lipid Metabolism* 1346.1 (1997): 75-85.
65. Lehmann, Fredrik, et al. "Discovery of inhibitors of human adipocyte fatty acid-binding protein, a potential type 2 diabetes target." *Bioorganic & medicinal chemistry letters* 14.17 (2004): 4445-4448.
66. Lan, Hong, et al. "Small-molecule inhibitors of FABP4/5 ameliorate dyslipidemia but not insulin resistance in mice with diet-induced obesity." *Journal of lipid research* 52.4 (2011): 646-656.
67. Berger, William T., et al. "Targeting fatty acid binding protein (FABP) anandamide transporters—a novel strategy for development of anti-inflammatory and anti-nociceptive drugs." *PloS one* 7.12 (2012): e50968.
68. Madsen, Peder, et al. "Molecular cloning and expression of a novel keratinocyte protein (psoriasis-associated fatty acid-binding protein [PA-FABP]) that is highly up-regulated in psoriatic skin and that shares similarity to fatty acid-binding proteins." *Journal of Investigative Dermatology* 99.3 (1992): 299-305.
69. Chmurzyńska, Agata. "The multigene family of fatty acid-binding proteins (FABPs): function, structure and polymorphism." *Journal of applied genetics* 47.1 (2006): 39-48.
70. Makowski, Liza, and Gökhan S. Hotamisligil. "The role of fatty acid binding proteins in metabolic syndrome and atherosclerosis." *Current opinion in lipidology* 16.5 (2005): 543.
71. Rolph, Michael S., et al. "Regulation of dendritic cell function and T cell priming by the fatty acid-binding protein AP2." *The Journal of Immunology* 177.11 (2006): 7794-7801.
72. Armstrong, Eric H., et al. "Structural basis for ligand regulation of the fatty acid-binding protein 5, peroxisome proliferator-activated receptor β/δ (FABP5-PPAR β/δ) signaling pathway." *Journal of Biological Chemistry* 289.21 (2014): 14941-14954.

73. Sanson, Benoît, et al. "Crystallographic study of FABP5 as an intracellular endocannabinoid transporter." *Acta Crystallographica Section D: Biological Crystallography* 70.2 (2014): 290-298.
74. van de Pavert, Serge A., and Reina E. Mebius. "New insights into the development of lymphoid tissues." *Nature Reviews Immunology* 10.9 (2010): 664-674.
75. Morgan, Elwin, Padmamalini Kannan-Thulasiraman, and Noa Noy. "Involvement of fatty acid binding protein 5 and PPAR/in prostate cancer cell growth." *PPAR research* 2010 (2010).
76. Tan, Nguan-Soon, et al. "Selective cooperation between fatty acid binding proteins and peroxisome proliferator-activated receptors in regulating transcription." *Molecular and cellular biology* 22.14 (2002): 5114-5127.
77. Liu, Rong-Zong, et al. "Association of FABP5 expression with poor survival in triple-negative breast cancer: implication for retinoic acid therapy." *The American journal of pathology* 178.3 (2011): 997-1008.
78. Levi, Liraz, et al. "Saturated fatty acids regulate retinoic acid signalling and suppress tumorigenesis by targeting fatty acid-binding protein 5." *Nature communications* 6 (2015).
79. Tölle, Angelika, et al. "Fatty acid binding proteins (FABPs) in prostate, bladder and kidney cancer cell lines and the use of IL-FABP as survival predictor in patients with renal cell carcinoma." *BMC cancer* 11.1 (2011): 1.
80. Bao, Zhengzheng, et al. "A Novel Cutaneous Fatty Acid-Binding Protein-Related Signaling Pathway Leading to Malignant Progression in Prostate Cancer Cells." *Genes & cancer* 4.7-8 (2013): 297-314.
81. Yang, Jing, et al. "Site-specific mapping and quantification of protein S-sulphenylation in cells." *Nature communications* 5 (2014).
82. Kane, Christopher D., and David A. Bernlohr. "A simple assay for intracellular lipid-binding proteins using displacement of 1-anilino-naphthalene 8-sulfonic acid." *Analytical biochemistry* 233.2 (1996): 197-204.
83. Meister, Alton. "Selective modification of glutathione metabolism." *Science* 220.4596 (1983): 472-477.
84. Meister, Alton. "Glutathione metabolism and its selective modification." *J Biol Chem* 263.33 (1988): 17205-17208.
85. Khalil, Ikramy A., et al. "Uptake pathways and subsequent intracellular trafficking in nonviral gene delivery." *Pharmacological reviews* 58.1 (2006): 32-45.
86. <https://www.addgene.org/viral-vectors/lentivirus/lenti-guide/>
87. <https://www.labome.com/method/siRNAs-and-shRNAs-Tools-for-Protein-Knockdown-by-Genes-Silencing.html>
88. http://www.bio-rad.com/webroot/web/pdf/lsr/literature/10-0826_transfection_tutorial_interactive.pdf
89. Mann, Matthias. "Functional and quantitative proteomics using SILAC." *Nature reviews Molecular cell biology* 7.12 (2006): 952-958.
90. Macek, Boris, Matthias Mann, and Jesper V. Olsen. "Global and site-specific quantitative phosphoproteomics: principles and applications." *Annual review of pharmacology and toxicology* 49 (2009): 199-221.
91. Sharma, Kirti, et al. "Ultradeep human phosphoproteome reveals a distinct regulatory nature of Tyr and Ser/Thr-based signaling." *Cell reports* 8.5 (2014): 1583-1594.
92. Bian, Yangyang, et al. "Ultra-deep tyrosine phosphoproteomics enabled by a phosphotyrosine superbinder." *Nature Chemical Biology* 12.11 (2016): 959-966.
93. Erve, John CL, et al. "Spectral accuracy of molecular ions in an LTQ/Orbitrap mass spectrometer and implications for elemental composition determination." *Journal of the American Society for Mass Spectrometry* 20.11 (2009): 2058-2069.
94. Jamur, Maria Célia, and Constance Oliver. "Permeabilization of cell membranes." *Immunocytochemical methods and protocols* (2010): 63-66.
95. Chan, Warren CW, and Shuming Nie. "Quantum dot bioconjugates for ultrasensitive nonisotopic detection." *Science* 281.5385 (1998): 2016-2018.
96. Petryayeva, Eleonora, W. Russ Algar, and Igor L. Medintz. "Quantum dots in bioanalysis: a review of applications across various platforms for fluorescence spectroscopy and imaging." *Applied spectroscopy* 67.3 (2013): 215-252.